Engineering Library

APPLICATIONS OF UNSTEADY STATE GAS FLOW CALCULATIONS

by

John D. Janicek and Donald L. Katz
University of Michigan

ABSTRACT

The unsteady state differential equation for flow of gas from reservoirs has been solved approximately for relatively large values of time by using a constant diffusivity. The solution gives the flowing sand-face pressure as a function of time for constant flow rate from an infinite reservoir.

A parallel development starting with the basic differential equation gives a series of relationships from an assumption that the rate of pressure decline is constant with respect to radius within the effective radius of drainage but changes as the effective radius of drainage increases. These relationships for known reservoir constants and Darcy flow include:

1. Rate of pressure decline of a flowing well as a function of flow rate and effective radius of drainage.
2. Pressure distribution in the reservoir for a given flow rate and effective radius of drainage.
3. The relationship between the effective radius of drainage where gas begins to flow toward the well bore and the Darcy apparent radius of drainage in the steady state Darcy equation.
4. The effective radius of drainage as a function of time.

Presented at Research Conference on "Flow of Natural Gas from Reservoirs", University of Michigan, June 30 - July 1, 1955.

Except for a mathematical constant, this development results in the same time-dependence of the sand-face pressure for relatively large values of time as the approximate mathematical solution mentioned above.

The relationship for time dependence of sand-face pressure in an infinite reservoir is used to predict the effect of the superposition of a series of successive flow transients on the sand-face pressure. Pressure build-up curves, apparent stabilization pressures, the exponent of back-pressure curves for normal and reversed sequence flows, time variation of the performance coefficient and the isochronal back-pressure test are discussed in light of the above relationship with superposition.

At this point in the paper the deviations from Darcy's law at high flow rates are incorporated into the equation for time dependence of sand-face pressure. A test procedure is suggested for obtaining the performance characteristics of gas wells, including time as a variable. Also, a procedure is given for calculating the performance characteristics of a gas well from core data including time as a variable.

APPLICATIONS OF UNSTEADY STATE GAS FLOW CALCULATIONS

The back-pressure curve is widely used for predicting the deliverability of a gas well. A well is opened to a flow rate and the well head pressure is allowed to stabilize to a slow rate of decline, if possible. The flow rate is then changed and the well again allowed to stabilize. The data are plotted as the difference in the squares of the closed-in pressure (p_f) and the flowing sand-face pressure (p_s) versus the flow rate, generally yielding a straight line on log-log paper of slope 1/n and intercept c. In many cases, however, the intercept c tends to decline as the time allowed for stabilization is increased and the value of n sometimes depends on whether or not the flow rates were changed in increasing order or in decreasing order.

In order to better understand the reactions to be expected of a reservoir, an idealized Darcy flow reservoir is studied first. The usual steady state Darcy laminar flow formula may be derived by setting the rate of pressure decline equal to zero, which in many cases may be applied with good accuracy to reservoir in a "pseudo"- steady state where the pressure drops very slowly. The effect of time as a variable may be approximated by deriving all the results from the simple assumption that the rate of pressure decline is a constant for all radii within a "radius of drainage". Although the rate of decline is assumed constant independent of radius, it is allowed to change as the radius of drainage moves out into the formation. The results are used to derive a back-pressure equation including the effects of deviations from Darcy's law with a procedure for evaluating the necessary constants from either well test data or from core data. It is shown that the prediction of deliverability while the radius of drainage is moving is different from the condition when it becomes stationary after reaching the boundary of the reservoir or because of well interference. Methods of handling these two regimes are indicated. In this paper steady decline is defined as the condition when the radius of drainage becomes constant and the pressure at the radius of drainage declines at essentially the same rate as the equalized average formation pressure within the effective radius of drainage.

DIFFERENTIAL EQUATION

The ideal gas reservoir under consideration is one of uniform permeability, porosity, and thickness. The gas is at a constant temperature with uniform viscosity, molecular weight, and compressibility factor. Flow is radial and where a bounded reservoir is under consideration, it is assumed to have a circular boundary with the well bore in the center.

A material balance around a differential volume yields the equation of continuity, in one dimension.

$$\frac{\partial(\rho v)}{\partial x} = -\phi \frac{\partial \rho}{\partial t} \tag{1}$$

Although Darcy's law for flow of gases through porous media may not apply at high flow rates[4][6], it is used in a simplified system and discussion is given later upon the significance of the deviations:

$$v = -\frac{k}{\mu} \frac{\partial p}{\partial x} \tag{2}$$

The equation of state is given by

$$\rho = \frac{p M}{z R T} \tag{3}$$

Combining the above equations for a radial system:

$$\frac{\partial^2 p^2}{\partial r^2} + \frac{1}{r} \frac{\partial p^2}{\partial r} = \frac{2 \mu \phi}{k} \frac{\partial p}{\partial t} = \frac{1}{\gamma} \frac{\partial p^2}{\partial t} \tag{4}$$

where $\gamma = k p/\mu \phi$ is commonly called the diffusivity.

Equation (4) may be written in the dimensionless form according to the scheme of Bruce, Peaceman, Rachford, and Rice[2] for radial flow.

$$\frac{\partial^2 P^2}{\partial R^2} + \frac{1}{R} \frac{\partial P^2}{\partial R} = \frac{\partial P}{\partial \Theta} = \frac{1}{2P} \frac{\partial P^2}{\partial \Theta} \tag{5}$$

For the most part, except for certain constants, the use of capital letters indicates dimensionless variables and lower case letters imply the use of consistent units unless the units are marked as a subscript.

METHOD OF FINITE DIFFERENCES

Electronic computers have been used to find numerical solutions of Equation (5) for the case of constant rate of production[2][10]. Cornell and Katz[4] applied the Schmidt method for solving the equation for generalized boundary and initial conditions. In order to do so, the non-linear coefficient (1/P) in Equation (5) was set equal to $(1/P_{average})$ for the particular case in order to remove the non-linearity. This is the same as using an average diffusivity γ in Equation (4).

The non-linearity in the basic differential equation may be taken into account with the graphical procedure, if desired, as illustrated with the following one-dimensional example. Equation (5) written as a finite difference equation in one-dimension becomes

$$\frac{2\,P\,\Delta^2 P^2}{(\Delta X)^2} = \frac{\Delta P^2}{\Delta \Theta} \tag{6}$$

Consider a general profile as shown in Figure 1 at some given time Θ and center attention on three general points 1, 2, and 3 which are separated by the distance ΔX. Let P_1^2, P_2^2, P_3^2 be points on the profile at time Θ, and let $P^2_{2,\Delta\Theta}$ be the new value of P_2^2 at the time $\Theta + \Delta\Theta$. Substituting these values into Equation (6) we have

$$P^2_{2,\Delta\Theta} - P_2^2 = P_2 \cdot \frac{2\,\Delta\Theta}{(\Delta X)^2}\,(P_3^2 + P_1^2 - 2\,P_2^2) \tag{7}$$

Now let

$$\frac{\Delta\Theta}{(\Delta X)^2} = \frac{1}{4} \tag{8}$$

Then

$$P_2^2 - P_{2,\Delta\Theta}^2 = P_2 \left(P_2 - \frac{P_1^2 + P_3^2}{2}\right) \tag{9}$$

Equation (9) shows that each increment in pressure decline as found by the usual Schmidt procedure[4][9] must be decreased by a factor equal to P_2, which is different for each point in the profile. In the usual procedure

$$P_{2,avg} \cdot \frac{\Delta\Theta}{(\Delta X)^2} = \frac{1}{4} \tag{10}$$

and

$$P_2^2 - P_{2,\Delta\Theta}^2 = P_2^2 - \frac{P_1^2 + P_3^2}{2} \tag{11}$$

Therefore

$$P_{2,\Delta\Theta}^2 = \frac{P_1^2 + P_3^2}{2} \tag{12}$$

Graphically, the point given by Equation (12) is given by the intersection of line joining P_1^2 and P_3^2 with the vertical line at "2". The correction may be applied by similar triangles by means of a ruler marked from zero to one. The zero mark is placed at P_2^2 on the curve and "one" is placed horizontally even with the point $(P_1^2 + P_3^2)/2$. A distance equal to P_2 is marked off on the ruler, and this point is projected horizontally to the point $P_{2,\Delta\Theta}^2$ directly below P_2^2. Although the construction lines are shown in Figure 1, most of them are unnecessary to be actually drawn.

The correction for the non-linearity may be applied to a radial flow system in the same way as described above. The procedure is similar to the one dimensional case[4][9] except that the radial distance is plotted on a logarithmic scale with the lines separated by ΔR. The uncorrected new

value of P_2^2 is found at the intersection of a line from P_1^2 to P_3^2 at the vertical line "2". This is corrected by multiplying the change in P_2^2 by the pressure at that point using the method of similar triangles.

The main advantage in the graphical procedure is the generality of the boundary and initial conditions which can be handled. Disadvantages lie in the fact that a large scale must be used in order for the finite difference approximation to be accurate and that the method does not provide an easy method for determining the characteristic constants of the gas reservoir.

APPROXIMATE ANALYTICAL SOLUTION

Consider the case of constant rate of production from an infinite reservoir. It has been shown that the effect of the non-linearity is to decrease the rate of pressure drop in proportion to the pressure. The correct solution to the non-linear differential equation should lie between the solutions of the corresponding linear equations using constant values for the non-linear coefficient (1/P) in Equation (5) (or the diffusivity γ in Equation (4)) equal to the highest and lowest values in the problem at hand, namely, $P_s \leq P \leq 1$. If P_c is the particular constant pressure used, the solution to the linear equation at the sand-face for large values of time and beginning from uniform shut-in conditions is given by[3][14]

$$P_f^2 - P_s^2 = \frac{Q}{4}\left[\ln\left(\frac{8\Theta P_c}{R_s^2}\right) - \delta\right] = \frac{Q}{4}\ln\frac{8\Theta P_c D^2}{R_s^2} \qquad (13)$$

or

$$(p_f^2 - p_s^2)_{psia^2} = \frac{1635\,\mu_{\bar{c}\bar{p}}\,\bar{z}\,T_{\circ R}\,q_{MCFD}\log\dfrac{5.93\times10^{-4}\,k_{md}\,p_{c,psia}}{\mu\,C_p\,\phi\,r_{s,ft}^2}\cdot t_{hr}}{k_{md}\,h_{ft}} \qquad (13a)$$

where γ is Euler's constant ($\gamma = 0.5772...$), $D^2 = e^{-\gamma}$, and Q is a dimensionless flow rate. The maximum error expected by using this equation as a solution of the non-linear differential equation corresponds to using the limiting values of P_c, giving

$$\text{Maximum error in } P_s^2 = \frac{Q}{4} \ln \frac{1}{P_s} \tag{14}$$

Thus, for $P_s = 0.85$ and $Q = 0.02$ the error in P_s^2 would be less than one tenth percent. This flow rate corresponds to almost 1,000 MCFD from a reservoir 10 feet thick, permeability of 100 md, 1000 psia pressure, and temperature of 100°F. Equation (13) is represented graphically in Figure 2. An approximate derivation of Equation (13) will be given using the concept of approximating unsteady state conditions by a succession of steady decline conditions. These steps in the derivation will yield some insight into the relationship between steady and unsteady states, the meaning of "radius of drainage", the rate of propagation of disturbances, and the relationship between finite and infinite reservoirs.

SUCCESSION OF STEADY DECLINE RESERVOIRS

Consider a bounded or finite reservoir producing at a constant rate. When the well is first opened the rate of pressure drop is very large, but after some time the rate of decline may become relatively small. If as a first approximation, the rate of pressure decline is set equal to zero then integration of Equation (5) yields the usual Darcy radial laminar flow formula

$$P_f^2 - P_s^2 = \frac{Q}{4} \ln \frac{R_a^2}{R_s^2} \tag{15}$$

where R_a and R_s are respectively the dimensionless Darcy apparent radius of drainage and sand-face radius, both of which are assumed fixed for the moment and at constant pressures. If the Darcy apparent radius of drainage, R_a, is given then the corresponding sand-face pressure P_s can be calculated for any flow rate Q. This Darcy pressure distribution is illustrated in Figure 3. One unsatisfactory characteristic of this equation is that it gives no information concerning the variation of the Darcy apparent radius of drainage with time. Strictly speaking, the derivation assumes that gas is entering and leaving the system at the same rate in order to maintain constant pressures throughout the reservoir. However, Muskat[13] and also MacRoberts[11] have used the Darcy pressure distribution together with a material balance to describe the change in the Darcy radius of drainage with time for certain boundary conditions.

In order to obtain an improvement on the Darcy formula for treating unsteady state problems, the concept of a steady decline reservoir is introduced. The usual definition of steady state implies no pressure variation with time. This condition should theoretically never be realized in a producing reservoir because of the material balance requirements. A single well in a bounded reservoir is defined as being in a condition of steady decline after the effect of the original drawdown has been felt in all parts of the reservoir and every point in the reservoir declines in pressure at the same rate as the average equalized pressure of the reservoir. It is recognized that this idealized approximation may not hold as well near the well bore as for points further out in the formation but it is felt that this approximation is a step forward from the Darcy condition of zero pressure decline and yields much semi-quantitative information which should be applicable to a large number of cases. This condition is also intuitively more satisfactory in that it satisfies the material balance for the total reservoir, in consistent units

$$q = \frac{\partial}{\partial t}\int_{r_s}^{r_b} \frac{\pi h M p}{z R_g T} d(r^2) = \frac{\pi h M}{z R_g T}\int_{r_s}^{r_b} \frac{\partial p}{\partial t} d(r^2) \qquad (16)$$

and

$$\frac{\partial p_{average}}{\partial t} = \frac{z R_g T}{\pi h M} \cdot \frac{q}{(r_b^2 - r_s^2)} \qquad (17)$$

Equation 17 states that for a reservoir of given properties and a given flow rate the rate of pressure decline depends only on the square of the boundary radius r_b. At this point the pressure gradient must be zero since there is no flow across this boundary. It seems plausible to assume that after a well is opened that the region near the well bore is affected first and that this region becomes larger with time. As a first approximation, it would seem that for each instant of time there should be a point at which gas has just begun to flow toward the well bore. At this point, where the net flow approaches zero as a limit, the pressure gradient is zero. This radius is very analogous to the bounding radius of a finite reservoir and this radius is called the effective radius of drainage, R_e, to distinguish it from the Darcy or apparent radius of drainage, R_a. These radii are illustrated in Figure 3 in dimensionless form. Since the effective radius of drainage has the same properties as a boundary radius, it follows that the average rate of pressure decline within this radius should be given by Equation 17 with r_e substituted for r_b. If at any instant of time the reservoir within the effective radius of drainage acts like a bounded reservoir in steady decline, then unsteady state decline may be pictured as a sequence of steady decline reservoirs bounded at r_e until r_e reaches the real boundary r_b and becomes stationary. This is illustrated in Figure 4. Equation 17 states that when r_e is very small then the rate of decline is very large, but as r_e becomes exceedingly large then the rate of decline becomes exceedingly small, explaining the apparent stabilization of the sand-face pressure some time after initiating flow. With these

approximations, it will be shown that the variation of the effective radius of drainage can be calculated as a function of time. The method will consist of setting the rate of pressure decline in Equation (5) equal to a constant and applying appropriate boundary conditions at R_e and R_s. It should be recognized at the outset that although mathematical reasoning is used to derive results based upon approximations relying on physical intuition, that the results cannot be expected to be mathematically rigorous in every respect. One inconsistency which will be pointed out is the failure of the approximation of the rate of pressure decline being independent of radius to hold well near the well bore for very steep pressure gradients. Another is that a reservoir obeying the differential Equation (5) should theoretically feel any disturbance at every point immediately upon opening the well. In the latter case, however, it is felt that physical intuition is as reliable as the mathematical description of the system. The idea of approximating an unsteady condition by a succession of steady conditions was suggested by Muskat[13].

RATE OF PRESSURE DECLINE, $\frac{dP}{d\Theta}$

The partial differential equation (5) may be transformed into the following ordinary differential equation if the rate of pressure decline is considered constant, using dimensionless variables

$$\frac{dP}{d\Theta} = \frac{1}{R^2} \cdot \frac{d^2P^2}{d(\ln R)^2} \tag{18}$$

The boundary conditions which must be satisfied are

$$\frac{d P^2}{d(\ln R)} = \frac{Q}{2} \quad \text{at} \quad R = R_s \tag{19}$$

$$\frac{d P^2}{d(\ln r)} = 0 \qquad \text{at} \quad R = R_e \tag{20}$$

These conditions follow from the fact that at the boundaries the flow rate is constant or steady and thus the profile must have the slope indicated by the radial laminar flow formula written for a differential section.

The first integration of Equation (18), considering the left hand member constant, together with the substitution of the boundary conditions given by Equations (19) and (20) gives not only the pressure gradient as a function of R but also permits the evaluation of the rate of pressure decline as a function of the effective radius of drainage.

$$-\frac{d P}{d \Theta} = \frac{Q}{R_e^2 - R_s^2} \tag{21}$$

or

$$-\frac{d p_{psia}}{d t_{hr}} = 0.375 \; \frac{z \, T_{°R} \, q_{MCFD}}{h_{ft} \, \phi \, (r_e^2 - r_s^2)_{ft^2}} \tag{22}$$

For a reservoir of $z = 0.9$, $T = 600°R$, $h = 40$ ft, $\phi = 0.24$, $q = 5000$ MCFD, the rate of pressure drop will be about 0.1 psia per hour when the effective radius of drainage has become about 1027 feet. Equation (22) is represented graphically in Figure 5. This rate of decline should hold fairly well near the sand-face if the pressure gradient is not too steep.

PRESSURE DISTRIBUTION

The pressure gradient obtained from the first integration is

$$\frac{d P^2}{d(\ln R)} = \frac{Q}{2} \left(1 - \frac{R^2 - R_s^2}{R_e^2 - R_s^2} \right) \tag{23}$$

Integration of Equation (23) gives the pressure profile which may be written in the following two forms, using P_f as the pressure at the effective radius of drainage and P_s as the pressure at the sand-face

$$P_f^2 - P^2 = \frac{Q}{4}\left[\left(1 + \frac{R_s^2}{R_e^2 - R_s^2}\right)\left(\ln \frac{R_e^2}{R^2}\right) - \frac{R_e^2 - R^2}{R_e^2 - R_s^2}\right] \qquad (24)$$

$$P^2 - P_s^2 = \frac{Q}{4}\left[\left(1 + \frac{R_s^2}{R_e^2 - R_s^2}\right)\left(\ln \frac{R^2}{R_s^2}\right) - \frac{R^2 - R_s^2}{R_e^2 - R_s^2}\right] \qquad (25)$$

Adding the above equations, the relationship between the pressure at the effective radius of drainage and the pressure at the sand-face of the well bore is obtained:

$$P_f^2 - P_s^2 = \frac{Q}{4}\left[\left(1 + \frac{R_s^2}{R_e^2 - R_s^2}\right)\left(\ln \frac{R_e^2}{R_s^2}\right) - \delta\right] \qquad (26)$$

where $\delta = 1$ according to this derivation. We shall later use δ = Euler's constant = 0.5772 instead of unity while the radius of drainage is moving in order for our final results to agree with Equation 13, and then use $\delta = 1$ after the effective radius of drainage reaches the outer boundary.

P_f ($= p_{f'}/p_f = 1$ ordinarily) is used here rather than unity as the pressure at the effective radius of drainage since Equations (24), (25), and (26) are valid even after the effective radius of drainage reaches the outer boundary of the reservoir, after which the pressure, $p_{f'}$, at the boundary also declines with time. Figure 6 gives a generalized graphical representation of the pressure distribution derived from Equation (24) for a steady decline reservoir when $r_e^2/r_s^2 > 100$ and for $\delta = 1$. To obtain the pressure distribution while the effective radius of drainage is moving, it is suggested to

use Figure 6 or Equation (24) at distances relatively far from the well bore where the approximation of $\mathcal{S} = 1$ and steady decline should be more accurate, and to use Equation (25) with the value of p_s from Figure 2 near the well bore to take into account the substitution of $\mathcal{S} = 0.57722$ while r_e is moving. This is equivalent to correcting the values of $(P_f^2 - P^2)/Q$ read from Figure 6 for radii near the well bore by adding a value of $(1 - 0.57722)/4 = 0.105695$. This should be quite accurate since Equation (25) reduces to the expected Darcy distribution near the sand-face for a given value of p_s. Figure 6 may be used directly after the effective radius of drainage becomes constant and steady decline begins. The figure shows that for a steady decline reservoir the difference in the squares of the outer boundary pressure and the sand-face pressure, $(p_{f'}^2 - p_s^2)$, remains constant with time. Figure 7 shows example profiles before and after the effective radius of drainage reaches the outer boundary.

THE RATIO R_e/R_a

To find the relationship between the effective radius of drainage, R_e, where fluid just begins to flow, and the apparent radius of drainage, R_a, used in the Darcy laminar flow formula equate Equations (15) and (26) under conditions where the effective radius of drainage is much larger than the sand-face radius. We find that

$$\ln \frac{R_e^2}{R_a^2} = \mathcal{S} \tag{27}$$

Let us define

$$D = \frac{R_a}{R_e} = \frac{r_a}{r_e} = e^{-\frac{\mathcal{S}}{2}} \tag{28}$$

Thus, it may be seen that when $R_e \gg R_s$ then R_e is directly proportional to R_a. If $\delta = 1$, then $D = 0.606$ and if $\delta = 0.5772$, then $D = 0.749$. The usual laminar flow formula, Equation (15), can be rewritten in the following form under these conditions:

$$P_f^2 - P_s^2 = \frac{Q}{4} \ln \frac{D^2 R_e^2}{R_s^2} \tag{29}$$

Note that Equation (29) holds even after R_e reaches the outer boundary and steady decline begins, stating that the difference in squares of the outer boundary pressure and the sand-face pressure is constant during steady decline. The declining boundary pressure P_f should be used when $R_e = 1$. Using a value of $\delta = 1$ during steady decline, Equation (28) states that the apparent radius of drainage in the usual laminar flow formula stabilizes to about six-tenths of the outer boundary radius. The variation of R_a/R_e with R_e is illustrated schematically in Figure 8. No attempt is made to predict the ratio in the transition regions at either end of the curve.

TIME DEPENDENCE OF THE SAND-FACE PRESSURE P_s: INFINITE RESERVOIR

The time dependence of the sand-face pressure can be found by eliminating R_e between Equation (21), applied at the sand-face, and Equation (29) and integrating. Using Equation (29) rather than Equation (26) in effect neglects the time required for R_e to become much greater than R_s. The integration can be carried out directly in terms of error functions which may then be expanded by semi-convergent series to give a result similar to Equation 13, under certain conditions.

$$P_f^2 - P_s^2 = \frac{Q}{4} \ln \left(\frac{8 \Theta P_s}{R_s^2} \cdot \frac{D^2}{F_s} + \frac{P_s F_f}{F_s} \right) \tag{30}$$

where

$$F = 1 - \left(\frac{Q}{8P^2}\right) + (1)(3)\left(\frac{Q}{8P^2}\right)^2 - (1)(3)(5)\left(\frac{Q}{8P^2}\right)^3 + \ldots . \qquad (31)$$

The subscript of F indicates what pressure to insert. Equation (30) reduces to Equation 13 for large values of time if $F \cong 1$ and P_c is used instead of P_s. This result may be obtained more directly by carrying out the integration using an average pressure P_c such that

$$\frac{dP_s}{d\Theta} \cong \frac{1}{2P_c}\,\frac{dP_s^2}{d\Theta} \qquad (32)$$

The integration yields

$$P_f^2 - P_s^2 = \frac{Q}{4} \ln\left(\frac{8\Theta P_c D^2}{R_s^2} + 1\right) \qquad (33)$$

Equation (33) reduces directly to Equation (13) for large values of time, provided we use $\delta = -\ln D^2 = 0.5772$ instead of the $\delta = 1$ derived in Equation (26). Figure 2 gives the graphical representation for large values of time. According to Equation 26, time should be large enough so that $R_e^2/R_s^2 = 8\Theta P_c/R_s^2 > 100$ for 1% accuracy in $P_f^2 - P_s^2$. The equality follows from Equations (13) and (29).

TIME DEPENDENCE OF THE EFFECTIVE RADIUS OF DRAINAGE, R_e

Comparison of Equations (13) and (29) yields the effective radius of drainage as a function of time for large values of time

$$R_e^2 = 8\Theta P_c \qquad (34)$$

This is the same as the fraction of the area bounded by r_b which has felt the disturbance, since the dimensionless radius of the outer boundary $R_b = 1$. The area drained at a given time is essentially independent of the flow rate

and depends only upon the properties of the reservoir and fluid. For a given reservoir the area of drainage is dependent only on time so long as the pressure level is essentially constant. The rate of propagation of the effective radius of drainage is seen to depend essentially on the diffusivity constant γ of the basic Equation (4) and the radius of drainage or time

$$\frac{d r_e}{d t} = \frac{4 \gamma}{r_e} \quad \text{in consistent units} \tag{35}$$

and

$$r^2_{e,ft} = \frac{1.056 \times 10^{-3} \, k_{md} \, p_{c,psia}}{\mu_{cp} \, \phi} \cdot t_{hr} \tag{36}$$

A similar, though not identical, result has been derived by MacRoberts[11] using a Darcy pressure distribution and constant sand-face pressure. Equation (36) is shown graphically in Figure 9. For a reservoir of 500 md, 2000 psia, 0.02 cp. viscosity, 0.24 porosity, the example for which the effective radius of drainage was 1027 ft. for a rate of decline of 0.1 psia per hour, the time required to reach this decline rate is about 4.67 hours. For a reservoir of 1 md, 450 psia, 0.015 cp viscosity, 0.12 porosity, the effective radius of drainage will be only about 80 feet after one day. Note from Equation (35) that the rate of increase of the effective radius is inversely proportional to the magnitude of the radius already attained.

TIME DEPENDENCE OF SAND-FACE PRESSURE, P_s: FINITE RESERVOIR

When a well is opened at a constant rate of production the unsteady state condition may be described by a succession of steady decline reservoirs bounded at the effective radius of drainage. This succession continues until the effective radius of drainage reaches the real boundary of the reservoir, after which steady decline ensues. In this analysis, it is assumed that the movement of the effective radius of drainage occurs as if the reservoir were

infinite until the outer boundary is reached, whereupon steady decline abruptly begins. Actually, the transition will probably begin gradually as the effective radius of drainage approaches the real outer boundary. For large values of time Equation (13) may be used to estimate the sand-face pressure as a function of time. The time required for the effective radius of drainage to reach the edge of the reservoir may be estimated from Equation (34) or Equation (36).

After steady decline begins the pressure at the outer boundary, P_f, also begins to decline. If Θ_b is defined as the time required for R_e to reach the outer boundary, then using Equation (21), P_f is obtained as a function of Θ, for $R_e \gg R_s$

$$1 - P_f = Q(\Theta - \Theta_b) \tag{37}$$

where

$$\Theta_b = \frac{1}{8 P_c} \tag{38}$$

If P_{sb} is the sand-face pressure when R_e just reaches the outer boundary then using Equations (29) and (37) to get P_s as a function of Θ during steady decline:

$$P_{sb}^2 - P_s^2 = 1 - P_f^2 = 2Q(\Theta - \Theta_b) + Q^2(\Theta - \Theta_b)^2 \tag{39}$$

where

$$P_{sb}^2 = 1 - \frac{Q}{4} \ln \frac{D^2}{R_s^2} \tag{40}$$

P_f declines linearly with time but P_s^2 declines directly proportional to P_f^2. A simplified procedure for computing the sand-face pressure would be to use Figure 2, allowing the boundary pressure $p_{f'}$ to vary with time and using a constant effective radius of drainage equal to the actual boundary radius. The problem is then reduced to using Figure 2 both before and after the effective radius of drainage reaches the boundary, provided $p_{f'}$ is used after until the radius of drainage reaches the known maximum. The time, t_b, is required for r_e to reach the outer boundary. Figure 8 or Equation (36) in the following form gives the time, t_b:

$$t_{b_{hr}} = \frac{\mu_{cp} \phi r_b^2}{1.056 \times 10^{-3} k_{md} p_{c,psia}} \tag{41}$$

After the time t_b, Figure 10 or Equation (22), in the following form may be used to compute $p_{f'}$:

$$p_f - p_{f'} = \frac{0.375 \; z \; T_{°R}}{h_{ft} \phi r_{b_{ft}}^2} (t_{hr} - t_{b_{hr}}) q_{MCFD} \tag{42}$$

It is suggested to use $D = r_a/r_e = 0.749$ while the effective radius of drainage, r_e, is moving, and to use $D = 0.606$ when r_e becomes stationary at the boundary r_b. It is emphasized that time may be used as a variable in Figure 2 only for times less than t_b.

It would seem that P_s could be found as a function of Θ directly by applying rate of pressure decline, Equation (21), directly at the sand-face. It seems, however, that this rate of decline, which is the same as the average rate of decline of the reservoir within the effective radius of drainage is more accurate when applied to points relatively distant from the sand-face where the pressure gradient is small and the pressure is nearer to that of the average reservoir pressure. Calculation of the decline of P_s by means of Equation (21) is actually slightly inconsistent with the method given above according to Equation (29) since it is assumed that P_f^2 and P_s^2 decline together, or

$$\frac{d P_s^2}{d\Theta} = \frac{d P_f^2}{d\Theta} \tag{43}$$

from which

$$\frac{d P_s}{d \Theta} = \frac{P_f}{P_s} \cdot \frac{d P_f}{d \Theta} \tag{44}$$

It is thus seen that the two methods of computing steady pressure decline at the sand-face become identical when flow rate is low enough that P_f/P_s is approximately unity. That inconsistent results can be derived merely emphasizes the fact that the original assumptions are not exactly consistent with the basic differential equation.

MULTI-WELL RESERVOIR: MAXIMUM EFFECTIVE DRAINAGE AREA PER WELL

As a first approximation assume that each well can be treated independently of all the other wells. The problem then is reduced to finding the maximum effective drainage area to be associated with each well. Unsteady state calculations could then be made as if the reservoir were infinite until the effective radius of drainage reaches the maximum effective drainage radius associated with the well, after which steady decline calculations could be made as for a reservoir bounded at the maximum radius of drainage.

One method of obtaining the area to use might be to take the geometrical area associated with each well converted into the equivalent circle. If S is the distance between wells and r_{em} is the maximum effective radius of drainage, then

$$r_{em} = \frac{S}{\sqrt{\pi}} \tag{45}$$

Another method is as follows. Define steady decline in a multi-well reservoir as the condition where the average rate of decline of each well is the same as that of every other well or of the reservoir as a whole. Assume that the entire reservoir has the same properties and that the total reservoir area is known to be of equivalent radius r_b. Then basing the dimensionless radius on this value of r_b and using Equation 21, we have at steady decline, neglecting the sand-face radius

$$\frac{Q_i}{R^2_{em_i}} = Q = \frac{dP}{d\Theta} \tag{46}$$

or

$$R^2_{em_i} = \frac{Q_i}{Q} = \frac{r^2_{em_i}}{r^2_b} = \frac{q_i}{q} \tag{47}$$

where "i" refers to the individual well and Q is the total reservoir production rate. The fraction of the total reservoir drained by a single well in steady

decline is equal to the fraction of the total reservoir production produced by that well. A good approximation might be to consider the geometrical area of a group of wells surrounding the well in question and then proportion the drainage area according to the flow rates. This method of proportioning areas was suggested by a paper by Matthews[12].

SUPERPOSITION OF SUCCESSIVE FLOW TRANSIENTS: INFINITE RESERVOIR

Superposition is a method of describing the net reaction of a system to a series of transients or impulses by adding together or superimposing the effects of the individual transients or impulses as if they acted independently of each other[8][14]. This principle may be applied to systems governed by linear differential equations. We have shown that the solution of our non-linear differential equation for a constant rate transient in an infinite reservoir may be approximated by the solution to a linear differential equation, Equation (13), within the maximum error given by Equation (14).

The case of a series of constant rate transients will be considered in which the well is opened to a constant flow rate for a period of time, then changed to a different constant flow rate for another period of time, and so on. The net impulse on the system with each change in flow rate is the net difference in flow rates, and each impulse causes a corresponding net change in the pressure observed at the sand-face. The total pressure drop at the sand-face may be calculated by adding the change in pressure due to each impulse acting through its respective net impulse time. For example, the total decrease in the square of the pressure at time Θ_2 due to the effects of two successive flows Q_1, Q_2, beginning respectively at times zero and Θ_1 is as follows, using Equation (13) with $P_c = 1$

$$P_f^2 - P_{s2}^2 = \frac{Q_1}{4} \ln \frac{8 D^2 \Theta_2}{R_s^2} + \frac{Q_2 - Q_1}{4} \ln \frac{8 D^2 (\Theta_2 - \Theta_1)}{R_s^2} \qquad (48)$$

or

$$P_f^2 - P_{s2}^2 = \frac{Q_1}{4} \ln \frac{8 D^2 \Theta_2}{R_s^2} + \frac{(-Q_1)}{4} \ln \frac{8 D^2 (\Theta_2 - \Theta_1)}{R_s^2}$$

$$+ \frac{Q_2}{4} \ln \frac{8 D^2 (\Theta_2 - \Theta_1)}{R_s^2} \qquad (49)$$

or

$$P_f^2 - P_{s2}^2 = \frac{Q_2}{4} \ln \frac{8 D^2 (\Theta_2 - \Theta_1)}{R_s^2} + \frac{Q_1}{4} \ln \frac{Q_2}{\Theta_2 - \Theta_1} \qquad (50)$$

Note from Equation (50) that the effect of the first flow period on the last becomes negligible when the total flow time becomes very large compared with the first interval. When the second term becomes negligible the equation reduces to the form of Equation (13) which states that the pressure at the sandface could be calculated as if the well were opened from shut-in conditions at the rate Q_2 for its net time of flow $(\Theta_2 - \Theta_1)$.

The physical meaning of superposition may be illustrated graphically by means of Figure 11. The total pressure drop given by Equation (48) may be further expanded into the three components given by Equation (49). The first term represents a production of rate Q_1 for the total time Θ_2 from the time the well was first opened, represented by ABD in Figure 11; the second term represents an injection of rate $(-Q_1)$ for the time $(\Theta_2 - \Theta_1)$ from the time the flow rate was changed at time Θ_1, represented by FH in the figure; the third term represents a production of rate Q_2 for the time $(\Theta_2 - \Theta_1)$ from the time the flow rate was changed, represented by FG in the figure. In other words, after the flow rate has been changed to Q_2 the system acts as if it were still producing Q_1 from the first flow which is cancelled by an injection of amount $(-Q_1)$ to give a net flow of Q_2. The algebraic sum of the three curves ABD, FH, and FG gives the net drawdown for the system, ABC. Superposition states that the net effect of a complicated series of changes in a single reservoir can be computed by taking the sum of the effects

on a number of independent reservoirs acting over the same period of time, each beginning in the same equalized condition. In our case: a single reservoir producing Q_1 until time Θ_1, at which time injection of Q_1 begins in another independent equalized reservoir to cancel the continued production of Q_1, and a production of Q_2 begins in a third reservoir. Note that once a reservoir is brought into the picture it must remain for the rest of the time, its net production being cancelled by another independent reservoir if necessary. It is seen that eventually the effects of injection and production of Q_1 will tend to cancel, curves FH and ABD, and the net effect will then be essentially Q_2 through its time period. Thus, FG and BC approach each other.

BUILD-UP CURVES

Superposition may be applied directly to the extrapolation of build-up curves obtained upon shutting in a well after a known period of flow, provided there is no well interference so that an infinite reservoir may be assumed. If a well producing Q_1 is shut in at time Θ_1, then the net impulse is $(-Q_1)$ and the pressure at time $(\Theta_2 - \Theta_1)$ from shut in is, using $P_c = 1$,

$$P_f^2 - P_{s2}^2 = \frac{Q_1}{4} \ln \frac{8 D^2 \Theta_2}{R_s^2} + \frac{(-Q_1)}{4} \ln \frac{8 D^2 (\Theta_2 - \Theta_1)}{R_s^2} \qquad (51)$$

$$= \frac{Q_1}{4} \ln \frac{\Theta_2}{\Theta_2 - \Theta_1} \qquad (52)$$

Thus, the square of the sand-face pressure versus the ratio of the total time to the time from shut-in plotted on semi-log paper should extrapolate as a straight line to the original shut-in pressure at unity on the time ratio scale as illustrated in Figure 12.

If the time of the first flow, Θ_1, is long with respect to the build-up time, $(\Theta_2 - \Theta_1)$ or if the sand-face pressure was changing very slowly prior to shutting the well in, the first term in Equation (51) may be considered as approximately equal to $P_f^2 - P_{s1}^2$ so that Equation (51) becomes:

$$\frac{(p_{s2}^2 - p_{s1}^2)_{psia}^2}{1000\, q_{l,MCFD}} = \frac{1.635\, \mu_{cp}\, z\, T_{°R}}{h_{ft}\, k_{md}} \log \frac{5.93 \times 10^{-4}\, k_{md}\, p_{c,psia}\, (t_2 - t_1)_{hr}}{\mu_{cp}\, \phi\, r_{s,ft}^2} \tag{53}$$

$$= A \log B\, (t_2 - t_1)_{hr} \tag{54}$$

where $(t_2 - t_1)_{hr}$ is the time measured after shutting in the well. Houpeurt[8] has suggested using Equation (53) for finding the permeability if all the other properties in the constant A are known. It is seen that if the left hand member of Equation (53) or (54) is plotted versus the logarithm of time in hours, then the slope is A, from which the permeability may be evaluated. In addition, however, the constant B may also be evaluated from the intercept of such a plot at $t_{hr} = 1$. Indeed, if a reservoir follows Darcy's law it would seem that this would be a very good method for testing a well to evaluate the constants of the reservoir, A and B, from build-up pressures taken as a function of time after shutting in a well which has been producing at a constant rate for a long period of time. The sand-face pressure would be declining at a very slow rate just prior to shutting in. This technique is illustrated in Figure 13.

APPARENT STABILIZATION PRESSURE

If a well is opened to a flow Q_1 for a period of time and then the flow rate is increased to Q_2, the sand-face pressure may appear to stabilize at a different value for the second flow period from that obtained by opening the well to the flow rate Q_2 beginning from equilibrium shut-in conditions and flowing for a time equal to the second flow period, as shown in Figure 14. If Θ_1 is the time of the flow Q_1, and Θ_2 is the total time for the successive flow test, then $P_f^2 - P_{s2}^2$ is given by Equation (50).

For the single flow test for a time Θ

$$P_f^2 - P_{s2}^2 = \frac{Q_2}{4} \ln \frac{8 D^2 P_c \Theta}{R_s^2} \qquad (55)$$

If the single flow test is allowed the same time to stabilize, Θ, as that of the successive flow test from the time of opening to the second flow, $\Theta_2 - \Theta_1$, it is seen by comparison of Equations (50) and (55) that the successive flow test will "stabilize" at a lower pressure than that of the single flow test, the difference in the square of the sand-face pressures for the two cases being the second term in Equation (50). This effect is confirmed by Haymaker, Binckley, and Burgess[7]. If the time for the second flow is large with respect to the first, then the second term in Equation (50) becomes small and the effect of the first flow period becomes small. Note that the effect of the first flow period depends not only on the time of the transient but also the magnitude of the flow rate. Thus, the "stabilized" pressures obtained on a successive flow test will depend not only on the time intervals chosen but also the magnitudes of the flow rates of all the preceding flow periods. Thus, the position and slope of a back pressure test using successive flows may depend not only on the time for each flow period but also on the magnitudes of the flow rates and the sequence used. This analysis assumes that the effective radius of drainage does not reach the extremity of reservoir during the test.

EXPONENT OF A NORMAL SEQUENCE BACK-PRESSURE PERFORMANCE CURVE

In the normal sequence back-pressure test the well is opened to successively larger flow rates and the apparent stabilized bottom hole sand-face pressure obtained for each flow rate. A plot of the difference in the squares of the reservoir equalized formation pressure and the bottom hole sand-face pressure versus the flow rate usually gives a straight line of slope 1/n on log log paper, represented by an equation of the form

$$q = c\,(p_f^2 - p_s^2)^n \tag{56}$$

where c is a constant which may be termed the performance coefficient or productivity index. The principle of superposition will be applied to determine whether or not the effect of using a successive flow test could influence the value of n obtained from the test even in a reservoir obeying Darcy's law. For the purpose of illustration of method and ease of mathematical manipulation, the conditions of the test will be chosen such that the duration of each flow period is the same and the flow rates are increased in the ratio of 1: 2:3...:k where k denotes the number of the flow period. The end of the successive time intervals may be denoted $\Theta_1 : 2\Theta_1 : 3\Theta_1 : \ldots k\Theta_1$, and the flow rates $Q_1 : Q_2 : \ldots : Q_k = Q_1 : 2Q_1 \ldots : kQ_1$. At the end of the first flow period we may write

$$P_f^2 - P_{s1}^2 = \frac{Q_1}{4} \ln \frac{8\,D^2\,\Theta_1}{R_s^2} \tag{57}$$

At the end of the third

$$P_f^2 - P_{s3}^2 = \frac{Q_1}{4} \ln \frac{8\,D^2\,(3\Theta_1)}{R_s^2} + \frac{(2Q_1 - Q_1)}{4} \ln \frac{8\,D^2\,(2\Theta_1)}{R_s^2}$$

$$+ \frac{(3Q_1 - 2Q_1)}{4} \ln \frac{8\,D^2\,\Theta_1}{R_s^2} \tag{58}$$

$$P_f^2 - P_{s3}^2 = \frac{3\,Q_1}{4} \ln \frac{8\,D^2\,\Theta_1}{R_s^2} + \frac{Q_1}{4} \ln 2 + \frac{Q_1}{4} \ln 3 \tag{59}$$

$$= \frac{Q_3}{4} \left[\ln \frac{8\,D^2\,\Theta_1}{R_s^2} + \frac{1}{3} \ln (3!) \right] \tag{60}$$

The results may be generalized for the kth flow period

$$P_f^2 - P_{sk}^2 = \frac{Q_k}{4}\left[\ln \frac{8\,D^2\,\Theta_1}{R_s^2} + \frac{1}{k}\ln(k!)\right] \qquad (61)$$

Note that Equation (61) states that the value of $(P_f^2 - P_s^2)$ obtained will be the same as if the test were a single flow test, given by the first term, plus an increase due to the preceding flow periods, given by the second term. For a series of single flow tests in a Darcy flow reservoir, the slope and the value of n should be unity and the dimensionless performance coefficient, C, should be the reciprocal of

$$\frac{1}{4}\ln \frac{8\,D^2\,\Theta_1}{R_s^2}$$

provided the same interval is used for each test beginning from equalized shut-in conditions. Such a test is called isochronal because of the equal flow periods from shut-in. It is seen from Equation (61) that on a plot of $\log (P_f^2 - P_s^2)$ versus $\log Q$ that as one proceeds from the lowest flow rate, corresponding to the first test in a successive flow test, to the highest flow rate that an increasing amount must be added to $(P_f^2 - P_s^2)$ of the isochronal flow test in order to correspond to the successive flow test. This has the effect of raising each point to a higher value as one proceeds to the right and thus the slope is increased above unity and the value of n decreased below unity. If Equation (56) is used to approximate Equation 61 then the value of n should be as follows, using the fact that $Q_k/Q_1 = k$, and evaluating n using the first and kth flow periods

$$n = \frac{\log k}{\log k\left[\dfrac{\ln\left(\dfrac{8\,D^2\,\Theta_1}{R_s^2}\right) + \dfrac{1}{k}\ln(k!)}{\ln \dfrac{8\,D^2\,\Theta_1}{R_s^2}}\right]} \qquad (62)$$

It is indeed a striking result that Equation (62) gives the values of n as substantially the same function of time over a wide range of time for a wide range of values of k. Figure 15 shows that the value of n tends to approach unity provided that the intervals of flow are sufficiently large, thereby diminishing the effect of the use of successive flows. It should be noted that the values of n obtained in this analysis was independent of the absolute magnitude of the flow rates used because of the special manner in which the ratios of the flow rates were chosen. A far more complicated function for n may be expected for arbitrary rates of flow and arbitrary flow intervals. This example illustrates the possibility of obtaining values of n less than unity for a normal sequence back-pressure test in a Darcy flow reservoir.

EXPONENT OF A REVERSE SEQUENCE BACK-PRESSURE CURVE

The principle of superposition will now be used to investigate the slope of the back-pressure curve for a reverse sequence test in which the well is opened to the largest flow rate first followed by successively smaller flow rates. The conditions of the test to be analyzed are that the flow intervals will again be the same for each flow rate and the comparative magnitudes of flow will be successively $Q_1/Q_2 = Q_2/Q_3 = Q_3/Q_4 = \ldots = Q_{k-1}/Q_k = 2$. Applying superposition for the third flow, we can obtain:

$$P_f^2 - P_{s3}^2 = \frac{Q_3}{4}\left[\ln\left(\frac{8D^2\Theta_1}{R_s^2}\right) + \frac{Q_1}{Q_3}\ln\frac{3}{2} + \frac{Q_2}{Q_3}\ln 2\right] \quad (63)$$

$$= \frac{Q_3}{4}\left[\ln\left(\frac{8D^2\Theta_1}{R_s^2}\right) + 2^2\ln\frac{3}{2} + 2\ln 2\right] \quad (64)$$

The results may be generalized for the kth flow interval

$$P_f^2 - P_{sk}^2 = \frac{Q_k}{4}\left[\ln\left(\frac{8\,D^2\Theta_1}{R_s^2}\right) + \sum_{m=1}^{m=k=1} 2^m \ln\left(\frac{m+1}{m}\right)\right] \qquad (65)$$

for $k > 1$

Equation (65) states that the values of $(P_f^2 - P_s^2)$ obtained in the reverse sequence test will be higher than that of an isochronal test by the amount indicated by the second term, the amount increasing with each successive flow. But since the sequence of the test is from high flow rates to low flow rates the deviation increases as we proceed from right to left on the usual log log plot of the back-pressure curve. This tends to decrease the slope and thus raise the value of n above unity. The value of n may be shown to be as follows, using the fact that $Q_1/Q_k = 2^{k-1}$, and using the first and kth flow periods to evaluate n.

$$n = \frac{\log 2^{k-1}}{\log 2^{k-1}\left[\dfrac{\ln \dfrac{8\,D^2\Theta_1}{R_s^2}}{\ln\left(\dfrac{8\,D^2\Theta_1}{R_s^2}\right) + \displaystyle\sum_{m=1}^{m=k-1} 2^m \ln\frac{m+1}{m}}\right]} \qquad (66)$$

It is again striking that Equation 66 gives the values of n as substantially the same function of time over a wide range of time for a wide range of values for k. Figure 16 shows that the values of n tends to decrease toward unity if the interval chosen for each flow period is sufficiently large, thereby diminishing the effect of the use of a successive flow test. It is emphasized again that other choices of flow rates and time intervals may give a far more complicated functional relationship for n. This example illustrates the possibility of obtaining values of n greater than unity for a reverse sequence test in a Darcy flow reservoir.

TIME VARIATION OF THE PERFORMANCE COEFFICIENT

The equation of the normal sequence back-pressure curve in dimensionless form may be written as follows:

$$Q = C (P_f^2 - P_s^2)^n \tag{67}$$

From Equation (67) it follows that C is the value of Q when $(P_f^2 - P_s^2) = 1$, which, in dimensionless form, corresponds to the absolute open flow condition. For the normal sequence test illustration given by Equation (61) the value of C may be obtained by setting $(P_f^2 - P_{sk}^2) = 1$. Let the value of k for which this is true be k', in which case $Q_{k'} = C = k' Q_1$. Q_1 is the value of the first flow rate, bearing in mind that in this example the actual test flow rates follow the pattern $Q_1 : Q_2 : \ldots Q_k = 1 : 2 : \ldots : k$. Then from Equation (61)

$$1 = \frac{Q_{k'}}{4} \left[\ln \frac{8 D^2 \Theta_1}{R_s^2} + \frac{1}{k'} \ln (k' !) \right] \tag{68}$$

or

$$1 = \frac{C}{4} \left[\ln \frac{8 D^2 \Theta_1}{R_s^2} + \frac{Q_1}{C} \ln \left(\frac{C}{Q_1} ! \right) \right] \tag{69}$$

Equation (69) is plotted in Figure 17 as essentially C as a function of time with Q_1 as a parameter. For a series of single flow tests giving an isochronal performance curve the second term vanishes and C declines with an increase in the flow period used as shown by the dotted line. If a successive flow test is used, the value of C depends not only on time but also on the absolute magnitude of the flow rates used. But again if large values of time are used for the flow intervals, the decline of C approaches that for the isochronal test and the effect of both the choice of the magnitude of the flow rates and the preceding transients becomes small.

ISOCHRONAL AND OTHER TEST PROCEDURES

Compare the form of the usual back-pressure curve equation with the unsteady state flow equation for constant production rate for a Darcy flow reservoir,

$$Q = C (P_f^2 - P_s^2)^n \tag{70}$$

$$Q = \left(\frac{4}{\ln \frac{8 D^2 \Theta_1}{R_s^2}} \right) (P_f^2 - P_s^2) \tag{71}$$

P_f^2 rather than unity in the dimensionless equations has been used above since the actual reservoir pressure used in these equations may be different from that used in originally evaluating the dimensionless groups. Equation (71) should describe an isochronal test in which each constant flow rate is run for the time Θ_1, the well then being shut in to equalized conditions before each flow period. Comparison of the two above equations show that for an isochronal test of a Darcy flow reservoir

$$n = 1 \tag{72}$$

$$C = \frac{4}{\ln \frac{8 D^2 \Theta_1}{R_s^2}} \tag{73}$$

The isochronal back-pressure test data of Cullendar[5] indicate, however, that n is generally less than unity. Although unsteady state calculations indicate some deviation of n from unity when a successive flow test is used, no such deviation is predicted for an isochronal test. The major assumptions used in this investigation are (1) the use of constant values for reservoir

characteristics, (2) neglecting the non-linearity of the basic differential equation, which depends primarily on the validity of (3) Darcy's law. For any given test, it would seem that use of average reservoir characteristics would not be too bad an assumption provided that the pressure drop was not too great or the flow rates too high. Within the error given by Equation (14) the use of a linear approximation to the non-linear differential equation should be all right. Houpeurt[8] has investigated the effect of changes in some properties on the value of n and has found them insufficient to explain large deviations of n from unity. He concludes that although Darcy's law may be valid for describing the flow of petroleum in porous media, it does not adequately describe the flow of gases because of the significant changes in kinetic energy due to the expansion and contraction of the gas in the irregular porous medium, described as turbulent flow by Cornell and Katz[4]. Houpeurt derives the following steady flow formula for flow between two fixed pressures at r_a and r_s in a radial system, in consistent units

$$p_f^2 - p_s^2 = \frac{\mu z R_g T q}{2 \pi h k M} \ln \frac{r_a^2}{r_s^2} + \frac{\zeta z R_g T q^2}{16 \pi^2 h^2 k r_s M} \qquad (74)$$

where ζ, zeta, is a characteristic of the porous medium. This is the same as the usual Darcy formula with the addition of the second term proportional to the square of the flow rate. Green and Duwez[6] and also Cornell and Katz[4] have used the quadratic form for expressing the pressure drop to take into account the deviations from Darcy's law

$$p_f^2 - p_s^2 = \frac{\mu z R_g T q}{2 \pi h k M} \ln \frac{r_a^2}{r_s^2} + \frac{\beta z R_g T q^2}{2 \pi^2 h^2 r_s M} \qquad (75)$$

where β is a characteristic of the porous medium. Comparison of equations (74) and (75) shows that

$$\zeta = 8 k \beta \qquad (76)$$

It is seen therefore that the results of the above researches are the same except for the description of a constant of the porous medium. Cornell and Katz[4] correlate β with an electrical resistivity factor F, related to the deviation of the flow path from a straight line, and a constant k_2 of the medium. If we make the rough approximations, $F = 4/\phi$ and $k_2 = 0.0283\,(k_{md}/\phi)^{3/4}$ derived from the work of Cornell and Katz, then we have

$$\beta = 3.89 \times 10^7 \frac{F}{k_2} \frac{1}{\sqrt{k_{md}\,\phi}} = \frac{5.5 \times 10^9}{k_{md}^{5/4}\,\phi^{3/4}} \qquad (77)$$

which is plotted in Figure 18. β can also be obtained by a flow test on a core. Houpeurt[8] illustrates the approximation of Equation (74) by an equation of the form of the usual back pressure curve, Equation 56, provided that the range of flow rates is not too great. Using Equation 34 converted to consistent units, giving the time variation of the effective radius of drainage, r_e, and Equation (28) for r_a/r_e we have for the performance coefficient

$$c = \left[\frac{1}{\lambda} \cdot \frac{2\pi h k M}{\mu z R_g T \ln \frac{r_a^2}{r_s^2}}\right]^n = \left[\frac{1}{\lambda} \cdot \frac{2\pi h k M}{\mu z R_g T \ln \frac{4 k p_c D^2 t}{\mu \phi r_s^2}}\right]^n \qquad (78)$$

where λ and n are numbers required to force the fit.

For the purposes of establishing constants by means of a back-pressure test Equation (75) and its exponential approximation may be written as follows, using Equations (28) and (36) to substitute time for the effective radius of drainage as a variable

$$\frac{(p_f^2 - p_s^2)_{psia^2}}{1000} = A\,q_{MCFD} \log B\,t_{hr} + C\,q_{MCFD}^2$$

$$= Aq_{MCFD} \log \frac{D^2 r_e^2}{r_s^2} + Cq_{MCFD}^2 \qquad (79)$$

$$q_{MCFD} = \left[\frac{1}{\lambda A \log B\, t_{hr}}\right]^n \left[\frac{(p_f^2 - p_s^2)_{psia^2}}{1000}\right]^n = c\left[\frac{(p_f^2 - p_s^2)_{psia^2}}{1000}\right]^n \qquad (80)$$

The reservoir characteristics equivalent to A, B, and C are given in the nomenclature. Equation (79) shows that A is the slope of a plot of $(p_f^2 - p_s^2)/1000\ q$ versus log t and the intercept is log (Cq + A log B) at $t_{hr} = 1$. This data may be obtained from pressure data taken as a function of time at a single flow rate. The time must be long enough so that the line from which A is evaluated represents times such that $(B\, t_{hr})/D^2 = r_e^2/r_s^2 > 100$ for 1% accuracy in $(p_f^2 - p_s^2)$, according to Equation 26. Note that although the deviation term in Equation (79) does not depend on time, it was derived with the understanding that $r_a \gg r_s$. and therefore the time must be large enough for this to be true. The constant C may be obtained by a series of isochronal drawdowns for several flow rates. A plot of $(p_f^2 - p_s^2)/q$ versus q has a slope equal to C provided the plot represents the same time from equalized shut-in conditions for all data points. The values of A and C then may be used with the intercept of the first plot (Cq + A log B) to obtain the value of B. With the value of B, a check should then be made to be sure that the constants were determined from data for which $\frac{B\,t}{D^2} > 100$. If this is not true then one should not expect the derived constants together with Equation (79) to represent the action of the reservoir for large values of time.

Isochronal data from at least two flow rates may be used to evaluate n in Equation (80),

$$n = \frac{\log \frac{q_2}{q_1}}{\log \frac{(p_f^2 - p_s^2)_2}{(p_f^2 - p_s^2)_1}} \qquad (81)$$

bearing in mind that the pressures in the above equation must represent the same time from equalized shut-in conditions for both flow rates. The other constants may be evaluated from data from a single drawdown in which the

pressure data is recorded as a function of time. Using the value of n obtained above the value of the performance coefficient

$$c = \frac{q}{\left[\frac{(p_f^2 - p_s^2)}{1000}\right]^n}$$

may be evaluated for each data point. Then since

$$\left(\frac{1}{c}\right)^{1/n} = \frac{(p_f^2 - p_s^2)_{psia^2}^{1/n}}{1000\, q_{MCFD}} = (\lambda A) \log B\, t_{hr} \qquad (82)$$

a plot of $(1/c)^{1/n}$ versus $\log t_{hr}$ will have a slope of (λA) and intercept $\lambda A \log B$ at $t_{hr} = 1$.

A method of testing using a pressure build-up curve might be developed for determining the reservoir constants as suggested for A and B by Equations (53) and (54) and by Figure 13 for a Darcy flow reservoir.

Equation (79) may be used even after the radius of drainage has stopped moving, if properly interpreted. Use of time as a variable assumes that the effective radius of drainage is still moving outward to its maximum value, discussed in the section pertaining to multiwell reservoirs, and that p_f is the constant formation pressure at the effective radius of drainage. The maximum radius of drainage r_{em} may be computed by, say, Equations (45) or (47), and the time, t_b, required to reach this maximum may be computed from Equation (34) or (38) given as follows in terms of the empirical constants

$$t_{b_{hr}} = \frac{D^2}{B} \frac{r_{em}^2}{r_s^2} \qquad (83)$$

After the time t_b Equation (79) may still be used, in the form using the constant radius of drainage r_{em} and substituting $p_{f'}$ for p_f, where $p_{f'}$ is the declining pressure at the outer boundary. This pressure may be predicted from Equation (22) or (37) in the following form:

$$\frac{(p_f - p_{f'})_{psia}}{(t - t_b)_{hr}} = \frac{1000\ A\ B}{4.606\ D^2} \cdot \frac{r_s^2}{(r_{em}^2 - r_s^2)} \cdot \frac{p_{f,\,psia}^2}{p_{c,\,psia}} \cdot q_{MCFD} \qquad (84)$$

Equation (84) states that the pressure at the maximum effective radius of drainage declines at the same rate as the average equalized pressure of the reservoir within the maximum radius of drainage. The use of Equation (79) after steady decline begins follows from Equation (26) which states that after the radius of drainage becomes fixed the difference in squares of the pressures at the outer boundary and at the well bore becomes constant. The problem then is to compute the decline of $p_{f'}$ from Equation 84, then calculate p_s from $p_{f'}$ by means of Equation (79).

EXAMPLE BACK-PRESSURE CURVE FROM TEST DATA

Figure 19 shows a plot of $(p_f^2 - p_s^2)/q$ versus q for a series of 3 hour drawdowns from the isochronal test data for Gas Well 3 taken by M. H. Cullender[5]. The slope of this line gives the value of $C = 1.32 \times 10^7$. Figure 20 gives a plot of $(p_f^2 - p_s^2)/q$ versus log t for a 214 hour drawdown in which the flow rate varied from 1229 MCFD at 1 hour to 1156 MCFD at 214 hours. The slope of this plot gives the value of A = 0.0108 and the intercept to be $0.0046 = A \log B + C\,q$. Using the value of A and C calculated above and a value of 1175 MCFD for q, we obtain a value of B = 2.577. Therefore, data should have been used for times greater than about 22 hours in order for $B\,t_{hr}/D^2 > 100$. Although annual 72 hour test data were available they were not used because of the long period between tests. The use of the three hour tests is questionable not only as to short time interval but also because they were taken 7 years after the long drawdown. The data were used for purpose of illustration. The back pressure equation in quadratic form may then be expressed as follows:

$$\frac{(p_f^2 - p_s^2)_{psia^2}}{1000} = 0.0108\, q_{MCFD} \log 2.577\, t_{hr} + 1.32 \times 10^{-7}\, q^2_{MCFD} \qquad (85)$$

with pressure in psia, flow rate in MCFD, and time in hours. Equation (85) is plotted in Figure 22. The effective radius of drainage is given by

$$\frac{r_e^2}{r_s^2} = \frac{B}{D^2}\, t_{hr} = 4.59\, t_{hr} \qquad (86)$$

In ten days the effective radius of drainage would be about 33 $r_{s,ft}$ if the reservoir obeyed Darcy's law and had uniform properties. Because of acidization or non-uniform properties r_s should be looked upon as some equivalent sand-face radius which may be many times the actual sand-face radius.

Using the usual form of the back-pressure curve, the value of n may be approximated from two three-hour drawdowns at different flow rates by means of Equation (81). For flow rates of 965 MCFD and 4,318 MCFD the values of $(p_f^2 - p_s^2)$ were respectively 10,190 and 48,960 $(psia)^2$, from which the value of n = 0.955. The values of n for all combinations of the three-hour runs ranged from 0.948 to 0.961 with an average value of 0.956. Using the long drawdown, the value of $(1/c)^{1/n}$ was calculated for each point by means of Equation (82) and plotted versus log t_{hr} in Figure 21. The slope gives the value of $\lambda A = 0.00767$. The intercept gives the value of

A log B = 0.0035. Using the value of λA above, the value of B = 2.86 is obtained which agrees fairly well with the B = 2.577 from the other method. Using the value of A from the first method $\lambda = 0.71$ is obtained. The back-pressure equation in exponential form is then

$$q_{MCFD} = \left[\left(\frac{1}{0.00767 \log 2.86\, t_{hr}}\right)\right]^{0.956} \left[\frac{(p_f^2 - p_s^2)_{psia^2}}{1000}\right]^{0.956} \qquad (87)$$

or

$$\frac{(p_f^2 - p_s^2)_{psia^2}}{1000} = 0.00767\, q_{MCFD}^{1.046} \log 2.86\, t_{hr} \qquad (88)$$

where flow rate is in MCFD, time in hours, and pressure in psia. This equation is plotted in Figure 22.

To suggest the effect of using a successive flow test for this well, assume a test as discussed in conjunction with Figure 15. If a three-hour successive flow test is used, then from Equation (86) $r_e^2/r_s^2 = 13.76$, and so $r_a^2/r_s^2 = 7.73$. Assuming that the dotted portion of the curve is approximately correct then the slope of the back-pressure curve would be about 0.80. This neglects deviations from Darcy's law.

EXAMPLE BACK-PRESSURE CURVE FROM CORE DATA

The back-pressure curve, Equation (75), may be written in the following form using time instead of the apparent radius of drainage as a variable,

$$\frac{(p_f^2 - p_s^2)_{psia^2}}{1000} = \frac{1.635\, \mu_{cp}\, z\, T_{°R}\, q_{MCFD}}{h_{ft}\, k_{md}} \log \frac{5.93 \times 10^{-4}\, k_{md} p_{c,psia}\, t_{hr}}{\mu_{cp}\, \phi\, r_{s_{ft}}^2} + \frac{1.09 \times 10^{-16}\, \beta\, M\, z\, T_{°R}\, q_{MCFD}^2}{h_{ft}^2\, r_{s_{ft}}} \qquad (89)$$

Green and Duwez[6] and also Cornell and Katz[4] give a method of measuring β by a laboratory test. For the purposes of this example, Equation 77 or Figure 18 is used to estimate β from the permeability and porosity. Consider the following characteristics:

p_f	= 3000 psia	T	= 140°F = 600°R
k	= 50 md	μ	= 0.015 cp
ϕ	= 0.12	z	= 0.9
h	= 20 ft	M	= 17.4 (0.6 gravity)
r_s	= 0.5 ft	β	= 2.03×10^8 ft^{-1}

The equation of the back-pressure curve then becomes

$$\frac{(p_f^2 - p_s^2)_{psia^2}}{1000} = 0.01324\, q_{MCFD} \log (197,000\, t_{hr}) + 1.037 \times 10^{-6}\, q^2_{MCFD} \tag{90}$$

The three-hour isochronal back-pressure curve is plotted in Figure 23.

CONCLUSIONS

The following procedure may be used for predicting the performance of a Darcy flow reservoir for a single drawdown from shut-in conditions provided that the reservoir constants are known. The two lumped constants, A and B, from flow tests or core data, the original formation pressure, p_f, the equivalent sand-face radius, r_s, and the outer boundary radius, r_b, are sufficient to evaluate all the groups used in the derived equations and charts. In a multiwell reservoir, Equations (45) or (47) may be used for computing the maximum effective radius of drainage, r_{em}, which may be used instead of r_b of the entire reservoir for the boundary radius to be associated with a particular well. Figure 2, which uses D = 0.749 in the dimensional constant, may then be used to predict the sand-face pressure, p_s, from the flow rate, q, and either time, t, or the effective radius of drainage, r_e, until the time, t_b, when the maximum radius of drainage is reached. The time, t_b, may be predicted from the maximum effective radius of drainage, r_{em}, by means of

Figure 9. This figure may also be used to predict the effective radius of drainage, r_e, for any other time less than t_b. For any given value of r_e the pressure profile or distribution may be computed directly from Figure 6 for points distant from the well bore but a correction of 0.105695 should be added to values of $(p_f^2 - p^2)/Q$ read for radii near the well bore to correct for using $\delta = 0.57722$ instead of $\delta = 1$ while r_e is moving. The rate of pressure decline may be found from Figure 5. This rate of decline should apply at the sand-face provided the pressure gradient is not too steep. After the time t_b the effective radius of drainage is assumed fixed at r_{em}. The pressure, $p_{f'}$, at the maximum radius of drainage may be computed as a function of time from Figure 10. Figure 6 may then be used to calculate p_s from the known value of r_s/r_e by using $p_{f'}$ instead of p_f in the figure. The figure may also be used to compute the entire pressure profile directly even near the well bore without making any corrections since $\delta = 1$ for a steady decline reservoir with constant r_e. Figure 2 may be used instead of Figure 6 to get the sand-face pressure during steady decline provided the abscissa is used in terms of radius of drainage, a value of D = 0.606 is used, and $p_{f'}$ is substituted for p_f.

The constants A, B, and C for use in the quadratic form of the back-pressure curve, Equation (79), or (λ A), B, and n for use in the exponential form, Equation (80), may be obtained from flow tests or from core data. These equations give the sand-face pressure as a function of flow rate, time, and the formation pressure, p_f or $p_{f'}$, at the effective radius of drainage. The movement of the effective radius of drainage may be predicted from Figure 9 and $p_{f'}$ may be predicted from Figure 10.

The principle of superposition may be used to find the net effect of a series of successive constant flow rate transients. Alternately, the graphical procedure of finite differences may be used to predict the effect of complicated boundary conditions in a Darcy flow reservoir if the constants A, B, r_s, r_b, and p_f are known.

NOMENCLATURE

Symbol

A empirical constant $= 2.303 \frac{\mu\ z\ R_g\ T}{2000\ \pi\ h\ k\ M} = \frac{1.635\ \mu_{cp}\ z\ T_{o_R}}{h_{ft}\ k_{md}}$

B empirical constant $= \frac{4\ D^2 k\ p_c}{\mu\ \phi\ r_s^2}$ Use appropriate q in consistent units or MCFD with A and C.

$= \frac{5.93 \times 10^{-4} k_{md} p_{c,psia}\ t_{hr}}{\mu_{cp}\ \phi\ r^2_{s,\ ft}}$ for D = 0.749

C empirical constant $= \frac{\beta\ z\ R_g\ T}{2000\ \pi^2 h^2\ r_s M} = \frac{1.09 \times 10^{-16}\ \beta\ M\ z\ T_{o_R}}{h^2_{ft}\ r_{s,ft}}$

C also dimensionless performance coefficient of Equation (70).

c usual performance coefficient, Equation (56).

D $r_a/r_s = e^{-\delta/2}$; 0.749 for $r_e < r_{em}$; 0.606 for $r_e = r_{em}$

F series factor defined by Equation (31).

F also resistivity factor

h thickness of the reservoir

k permeability

k also an index indicating the number of a successive flow test

k_2 reservoir constant connected with deviations from Darcy's law.

ln natural logarithm, base e.

log common logarithm, base 10.

L Overall length of a one-dimensional flow system.

M molecular weight

n exponent in the usual form of the back-pressure equation

p dimensional pressure

$p_f, p_{f'}$ respectively, the original equalized formation pressure and the formation pressure at the maximum radius of drainage, r_{em}, which may have dropped below the original pressure, p_f.

P dimensionless pressure, p/p_f

P_f unity or $p_{f'}/p_f$, whichever is appropriate.

Q dimensionless flow rate $= \dfrac{2\,\mu\, z\, R_g\, T}{\pi\, p_f^2\, k\, h\, M} \cdot q = \dfrac{2840\,\mu_{cp}\, z\, T_{^\circ R}}{p_f^2\, k_{md}\, h_{ft}} \cdot q_{MCFD}$

$$= \frac{4000\, A}{2.303\, p^2_{f,psia}} \cdot q_{MCFD}$$

Qθ fraction of the gas within the boundary r_b which has been removed.

r dimensional radius

R dimensionless radius = r/rb

R_g gas constant = 1545 using consistent units in ft-#mass-second system.

S distance between wells for square spacing.

t dimensional time

T absolute temperature, °R

v velocity

x linear dimensional distance

X dimensionless linear distance = x/L.

z compressibility factor

β reservoir constant accounting for deviations from Darcy's law used by Green and Duwez and Cornell and Katz, dimensions of length^{-1}

(Gamma) diffusivity constant $= \dfrac{k\,p}{\mu\,\phi} = 2.836 \times 10^{-4}\ \dfrac{k_{md}\, p_{psia}}{\mu_{cp}\,\phi}$, ft^2/hr

(Delta) Euler's constant = 0.5772 ....

also = -ln D^2 in which case it may be either 0.5772 or unity.

ϕ porosity

(lambda) constant to force quadratic form of back-pressure curve into usual exponential form

μ viscosity

ρ density

(zeta) reservoir constant for deviations from Darcy's law, used by Houpeurt, dimensions of length.

θ dimensionless time $= \dfrac{k\, p_f}{2\, \mu\, \phi\, r_b^2} \cdot t = 1.32 \times 10^{-4} \dfrac{k_{md}\, p_{f,psia}}{\mu_{cp}\, \phi\, r_{b,ft}^2} \cdot t_{hr}$

$= \dfrac{B}{8\, D^2} \cdot \dfrac{p_f}{p_c} \cdot \dfrac{r_s^2}{r_b^2} \cdot t_{hr}$

Subscripts

a apparent radius of drainage indicated by Darcy steady flow formula

b actual boundary radius usually, but the maximum effective radius of drainage may be substituted for it in a multiwell reservoir.

also, indicates that r_e has just reached r_b or r_{em}.

c average constant pressure used to eliminate non-linearity in the basic differential equation.

e effective radius of drainage

em maximum effective radius of drainage

f formation pressure at the effective radius of drainage

f' indicates that formation pressure at the effective radius of drainage, r_e, has dropped below the original pressure after r_e becomes constant.

i,k running index

m maximum

s sand-face.

REFERENCES

1. Aronofsky, J.S. and Jenkins, R., "A Simplified Analysis of Unsteady Radial Gas Flow", Trans. A.I.M.E., 201, 149 (1954).

2. Bruce, G.H., Peaceman, D.W., Rachford, Jr., H.H., and Rice, J.D., "Calculations of Unsteady-State Gas Flow Through Porous Media," J.Pet.Tech., 198, 79 (March 1953).

3. Carslaw, H.S., and Jaeger, J.C., Conduction of Heat in Solids, Oxford University Press, p. 283, 1947.

4. Cornell, D., and Katz, D.L., "Pressure Gradients in Natural Gas Reservoirs", J.Pet.Tech., 198, 61 (March 1953).

5. Cullender, M.H., "The Isochronal Performance Method of Determining the Flow Characteristics of Gas Wells", Paper No. 330-G, A.I.M.E., Dallas, Texas (1953).

6. Green, L., and Duwez, P.,"Fluid Flow Through Porous Metals", J. Appl. Mech., 18, 39 (1951).

7. Haymaker, E.R., Binckley, C.W., and Burgess, F.R., "Method of Establishing a Stabilized Back-Pressure Curve for Gas Wells Producing from Reservoirs of Extremely Low Permeability." Petroleum Trans., A.I.M.E., 186, 77 (1949).

8. Houpeurt, A., "Analogy of Radial Circular Transient Flow of Gases in Porous Media" Revue de L'Instituit Francais du Petrole et Annales des Combustibles Liquides, 8, No. 4, p. 129, No. 5, p. 193, No. 6, p. 248, (1953).

9. Jakob, M., Heat Transfer, Vol. I, John Wiley & Sons, New York, (1950).

0. Jenkins, R. and Aronofsky, J.S., "Unsteady Radial Flow of Gas Through Porous Media", J.Appl.Mech., 20, No. 2, 210 (June 1953).

1. MacRoberts, D.T., "Effects of Transient Conditions in Gas Reservoirs" Trans. A.I.M.E., 186, 36 (1949).

2. Matthews, Bronz, and Hazebroek, "Method for Determination of Average Pressure in a Bounded Reservoir", Petroleum Trans., A.I.M.E., 201, 182 (1954).

3. Muskat, M., Flow of Homogeneous Fluids, NcGraw-Hill Book Company, (1937).

4. Van Everdingen, A.F., and Hurst, W., "The Application of the Laplace Transformation to Flow Problems in Reservoirs." Petroleum Trans., A.I.M.E., 186, 305 (1949).

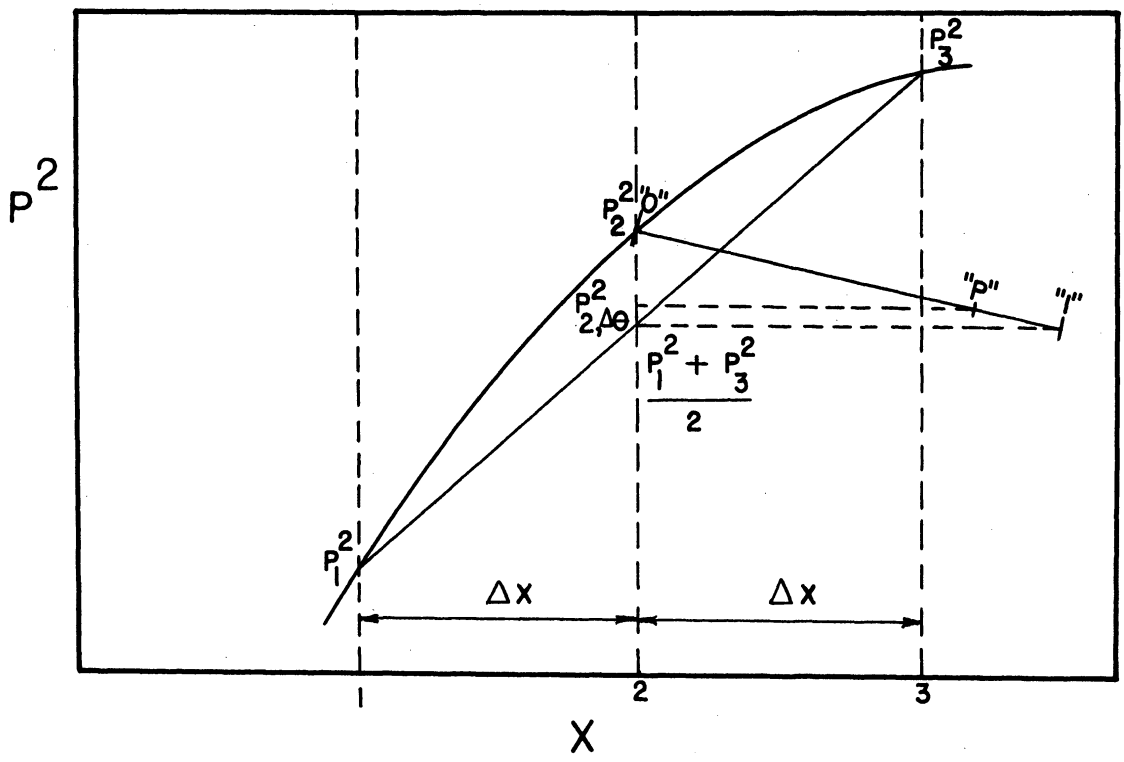


Figure 1. Solution of Non-Linear Differential Equation by Graphical Method of Finite Differences

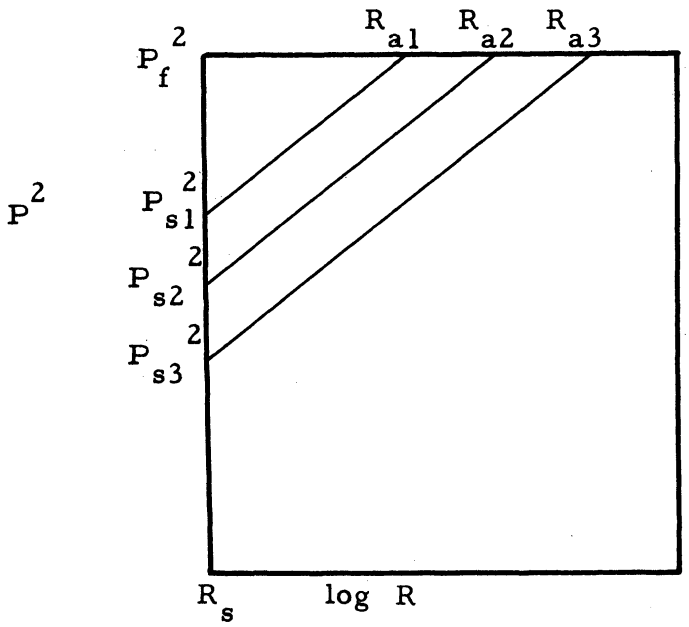


Figure 3. Darcy Pressure Distributions.

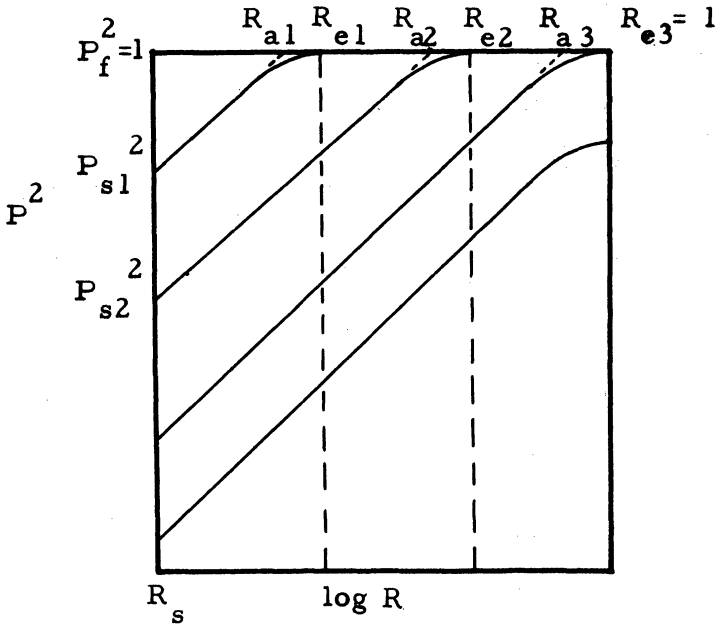
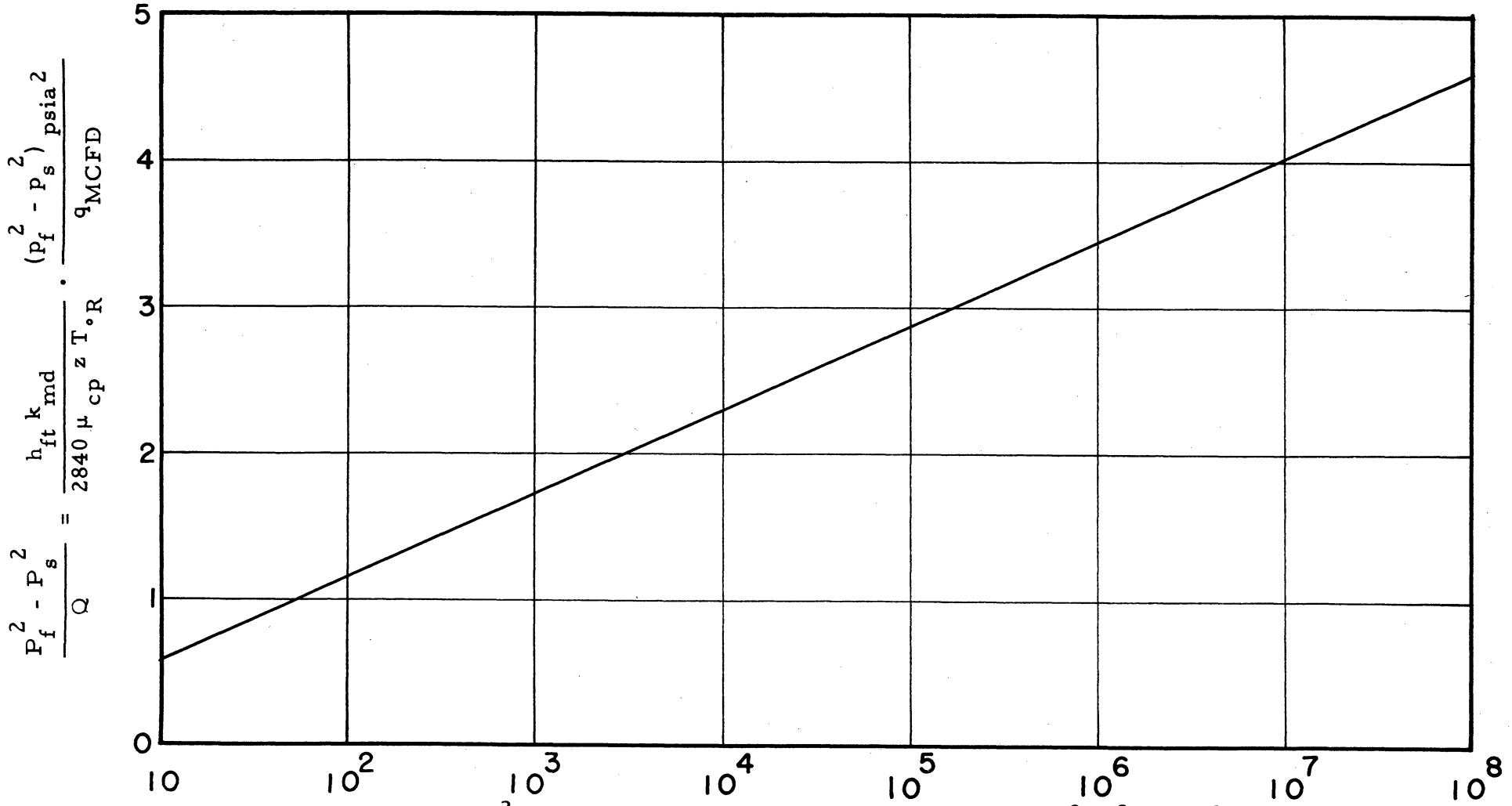


Figure 4. Pressure Distributions for a Succession of Steady Decline Reservoirs

Figure 2. Sand Face Pressure as a Function of Time or Radius of Drainage for Constant Rate of Production



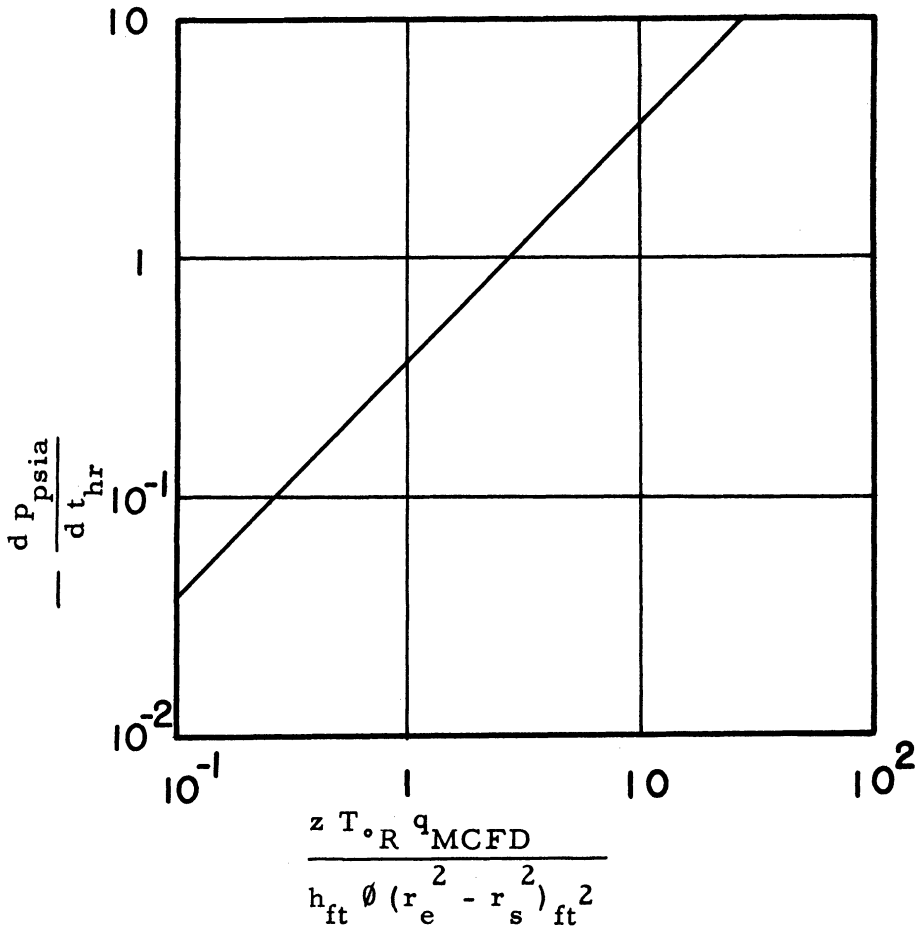


Figure 5. Rate of Pressure Decline Within the Effective Radius of Drainage, r_e, as a Function of r_e and the Flow Rate, q.

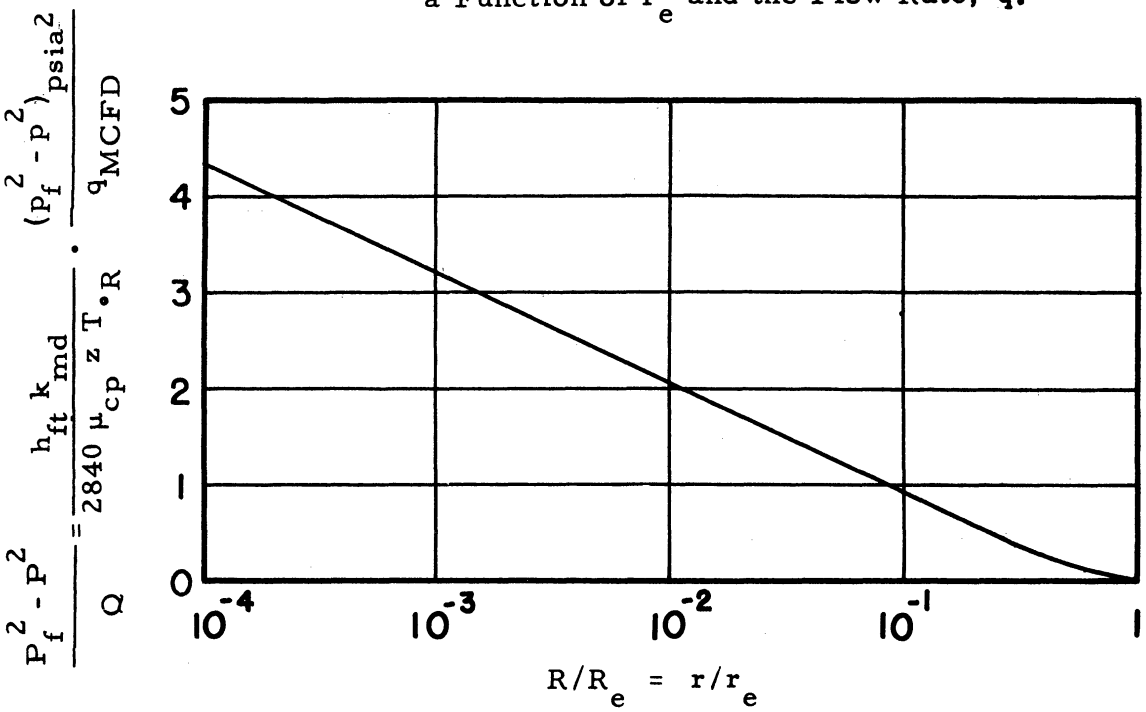


Figure 6. Generalized Pressure Distribution for $r_e^2/r_s^2 > 100$.

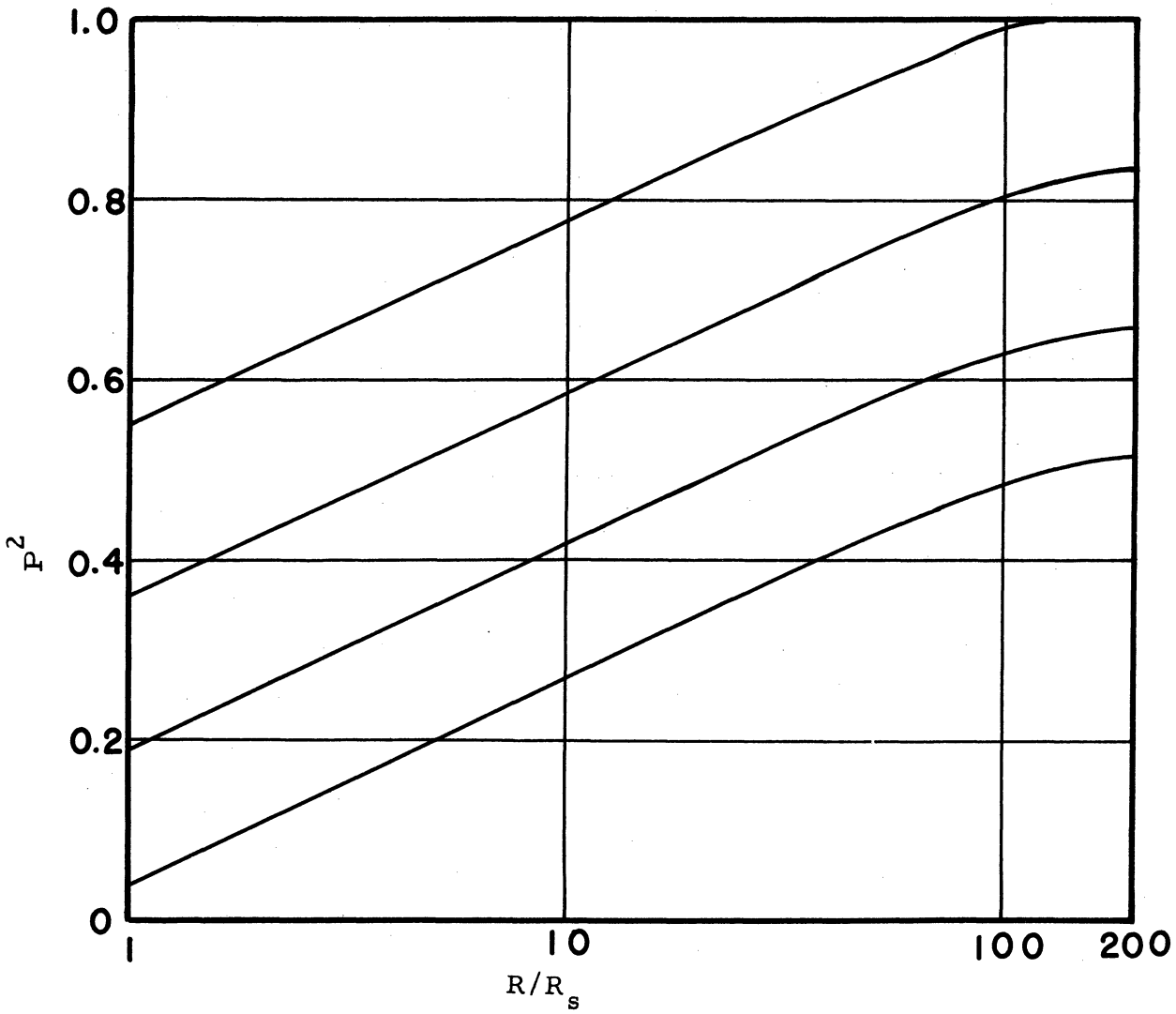


Figure 7. Example Dimensionless Pressure Distributions for $r_b/r_s = 200$ and $Q = 0.2$.

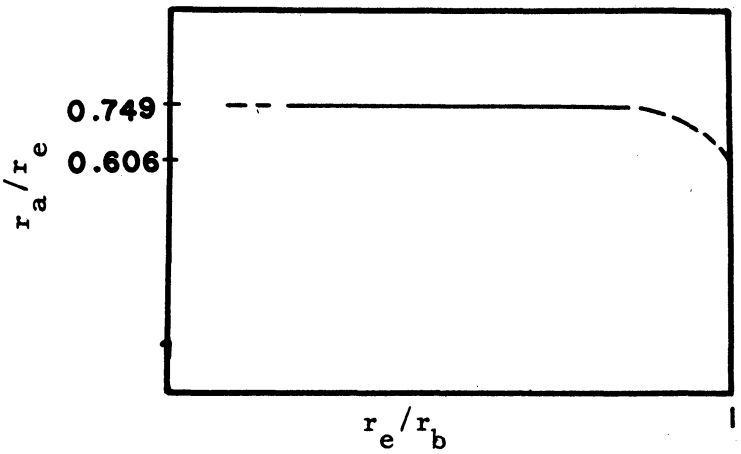


Figure 8. Ratio of the Darcy Apparent Radius of Drainage to the Effective Radius of Drainage, r_a/r_e.

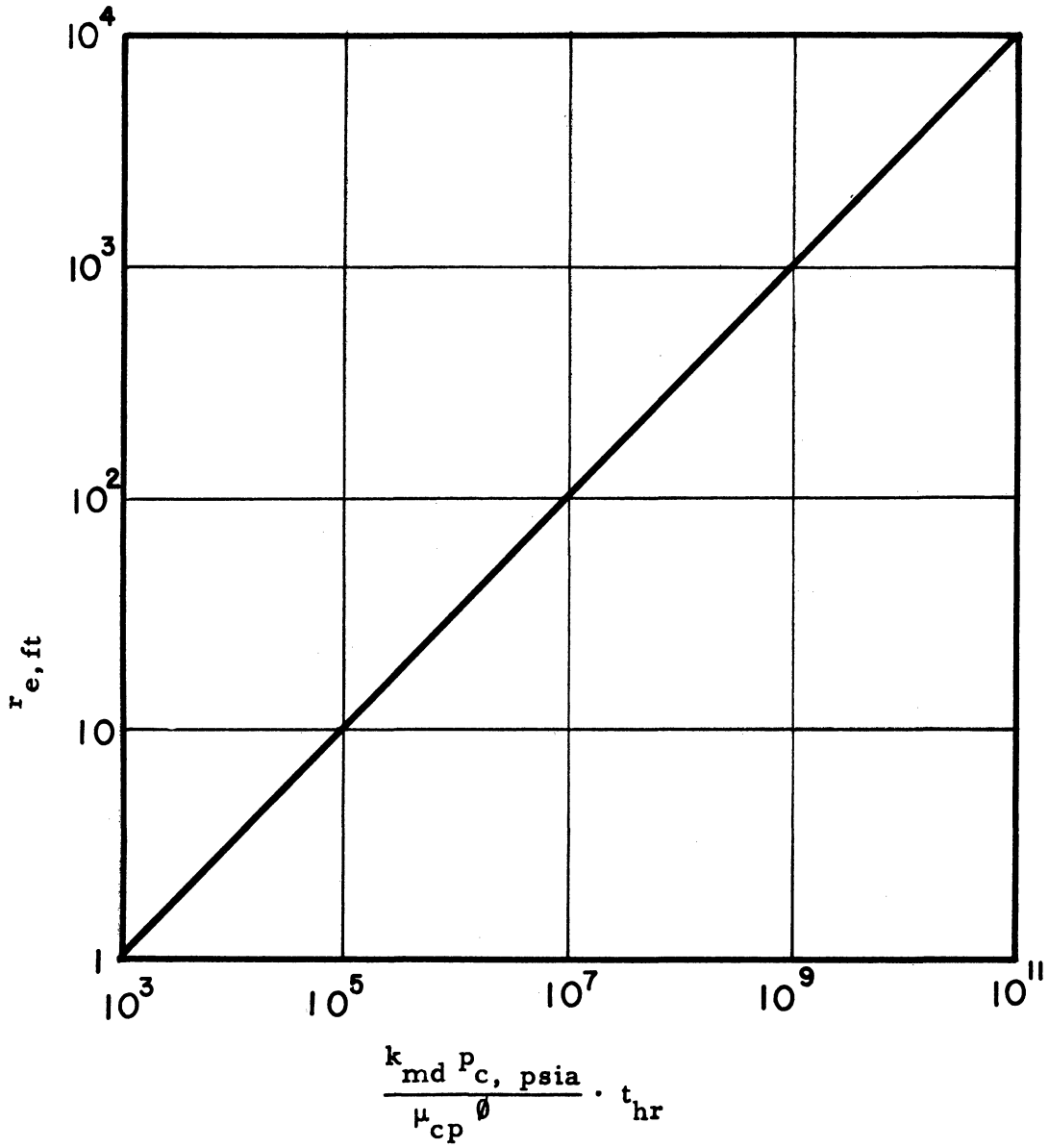


Figure 9. Effective Radius of Drainage, r_e, as a Function of Time, t, for an Infinite Reservoir.

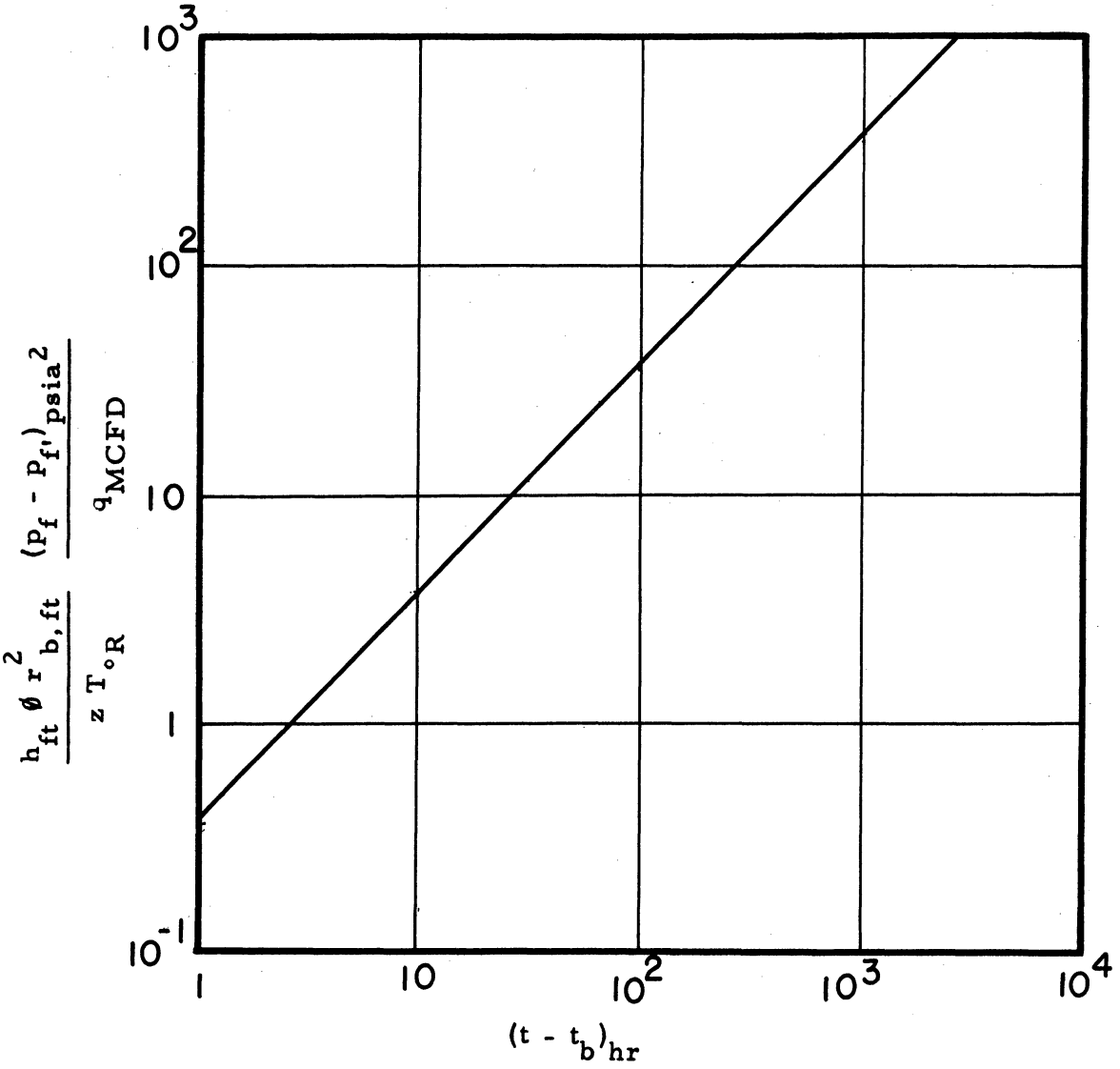


Figure 10. Boundary Pressure, $p_{f'}$, as a Function of the Total Time, t, and the Time, t_b, Required for r_e to Reach the Boundary, r_b. (Use r_{em} in This Figure for Multi-Well Reservoirs).

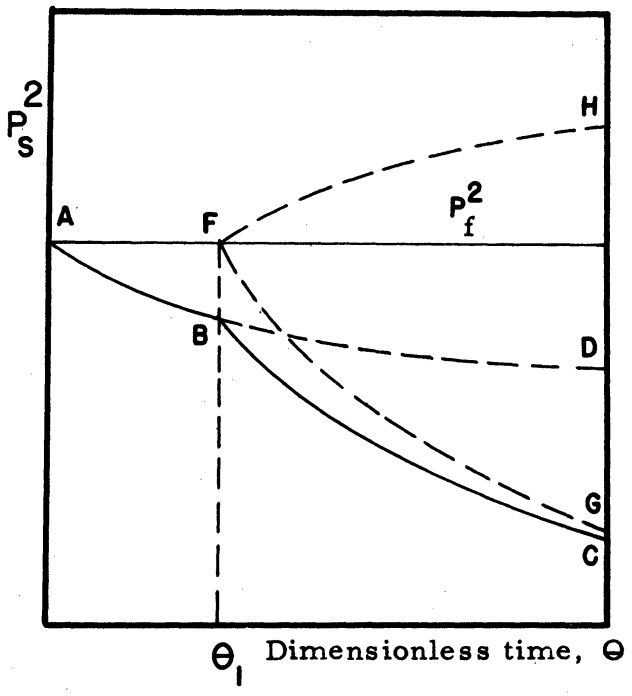


Figure 11. Effect of Superposition of Two Successive Flow Periods on the Sand-Face Pressure of an Infinite Darcy Flow Reservoir
ABD--Flow of Q_1 Only
FH --Injection of Q_1 Only
FG --Production of Q_2 Only
ABC--Net Superimposed Drawdown

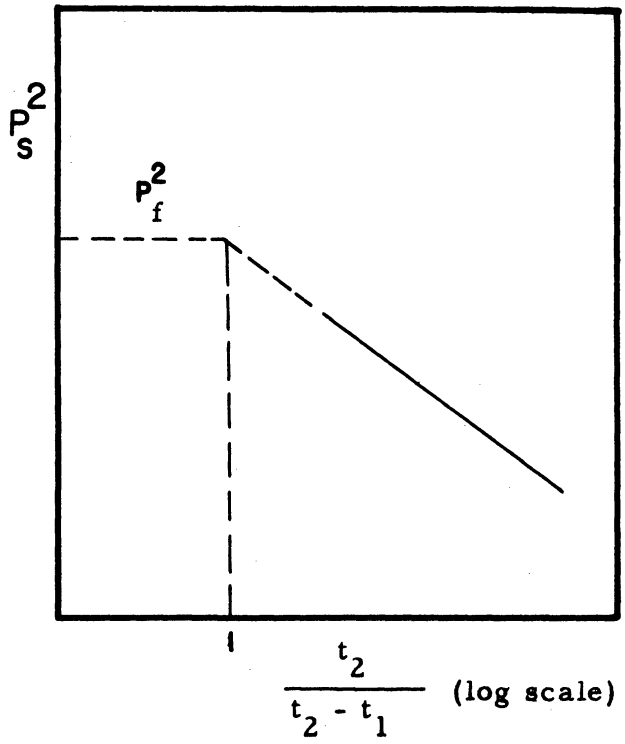


Figure 12. Extrapolation of Build-up Pressure Data to the Original Formation Pressure of a Darcy Flow Reservoir

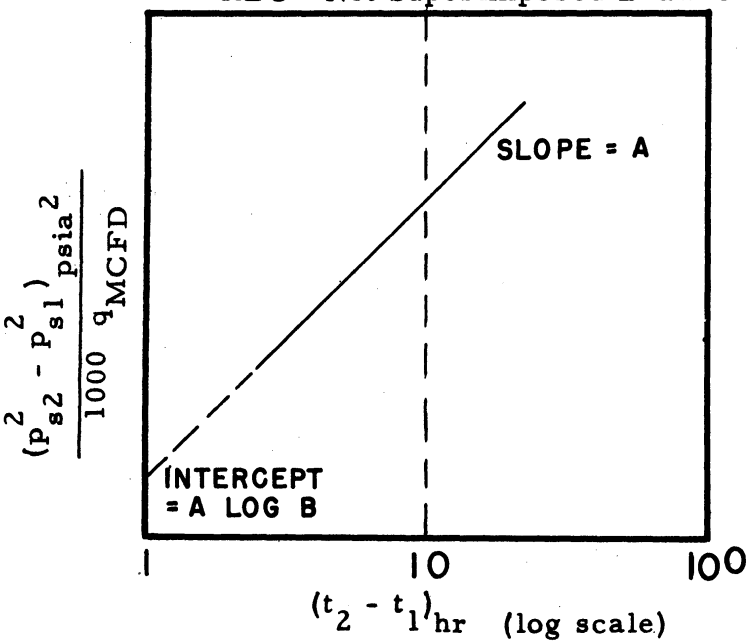


Figure 13. Use of Build-up Pressure Data to Evaluate Constants of a Darcy Flow Reservoir.

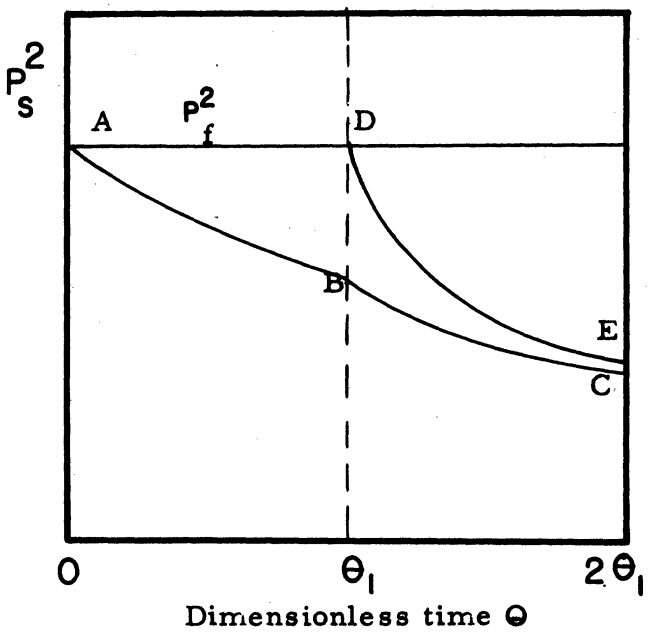
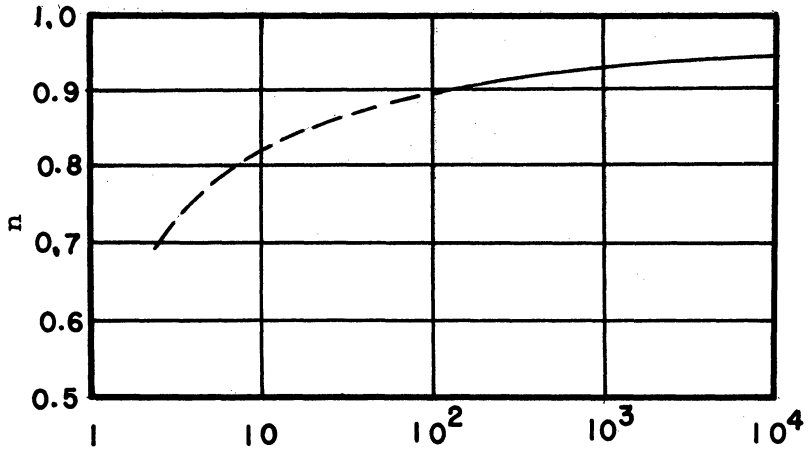
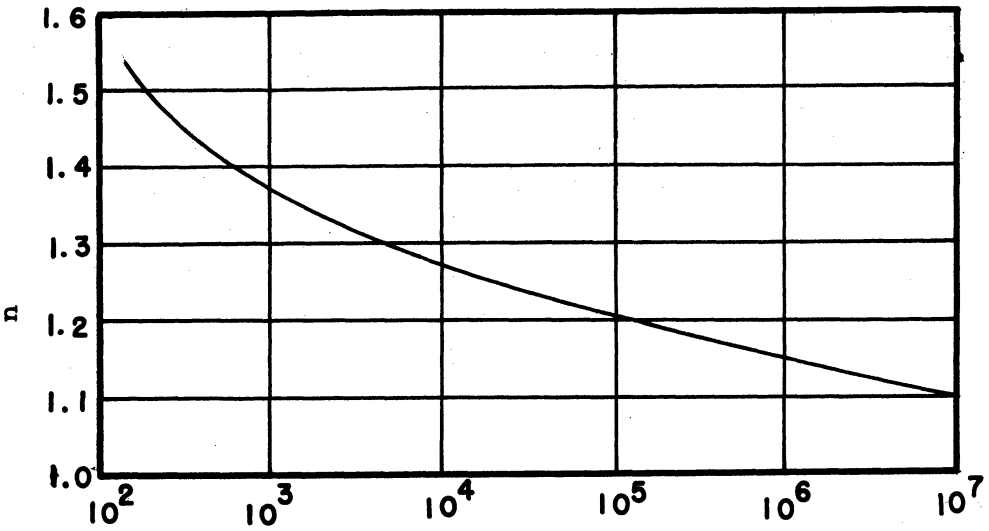


Figure 14. Comparison of Single Flow and Successive Flow Apparent Stabilization Pressures
ABC--Successive flow test: Q_1, Q_2.
DE --Single flow test: Q_2.



$$\frac{8\,D^2 P_c Q_1}{R_s^2} = D^2 \frac{r_{el}^2}{r_s^2} = \frac{r_{al}^2}{r_s^2}$$

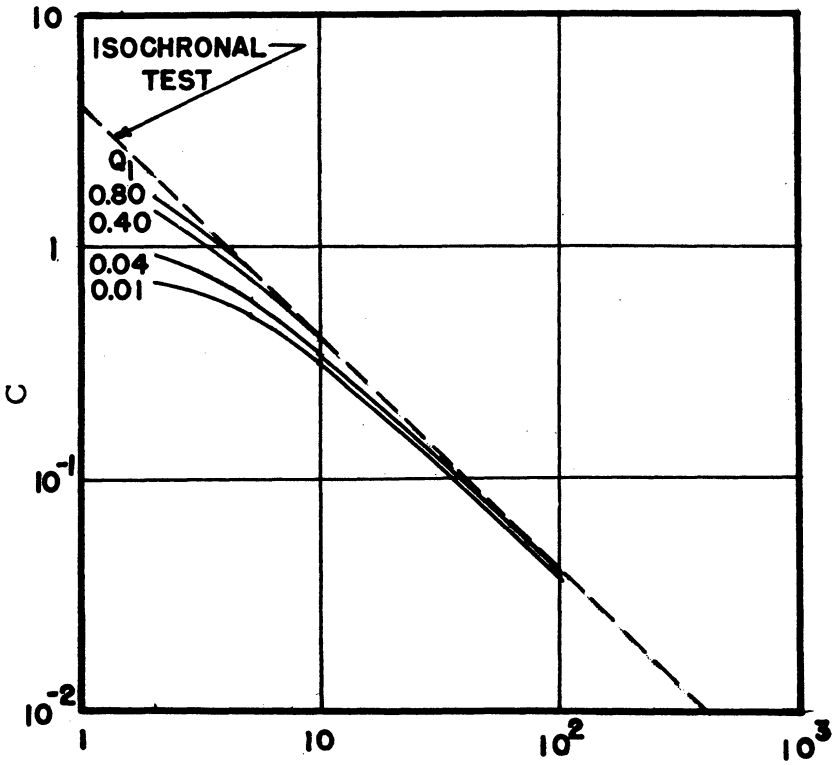
Figure 15. Effect of Superposition on Exponent, n, of a Normal Sequence Successive Flow Back Pressure Curve for Test Conditions: Equal Flow Periods, Θ_1, and Flow Rates Increasing as $Q_1:Q_2:Q_3:Q_4 = 1:2:3:4$



$$\frac{8\,D^2 P_c Q_1}{R_s^2} = D^2 \frac{r_{el}^2}{r_s^2} = \frac{r_{al}^2}{r_s^2}$$

Figure 16. Effect of Superposition on the Exponent, n, of a Reverse Sequence Successive Flow Back Pressure Curve for Test Conditions: Equal Flow Periods, Θ_1, and Flow Rates Decreasing as:

$$\frac{Q_1}{Q_2} = \frac{Q_2}{Q_3} = \frac{Q_3}{Q_4} = 2$$



$$\frac{8\,D^2\,P_c\,Q_1}{R_s^2} = D^2\,\frac{r_{el}^2}{\Psi_s^2} = \frac{r_{al}^2}{\Psi_s^2}$$

Figure 17. Effect of Superposition on the Dimensionless Performance Coefficient; C, of a Normal Sequence Successive Flow Back Pressure Curve for the Test Conditions: Equal flow periods, Q_1, and flow rates increasing as $Q_1 : Q_2 : Q_3 : Q_4 = 1:2:3:4$

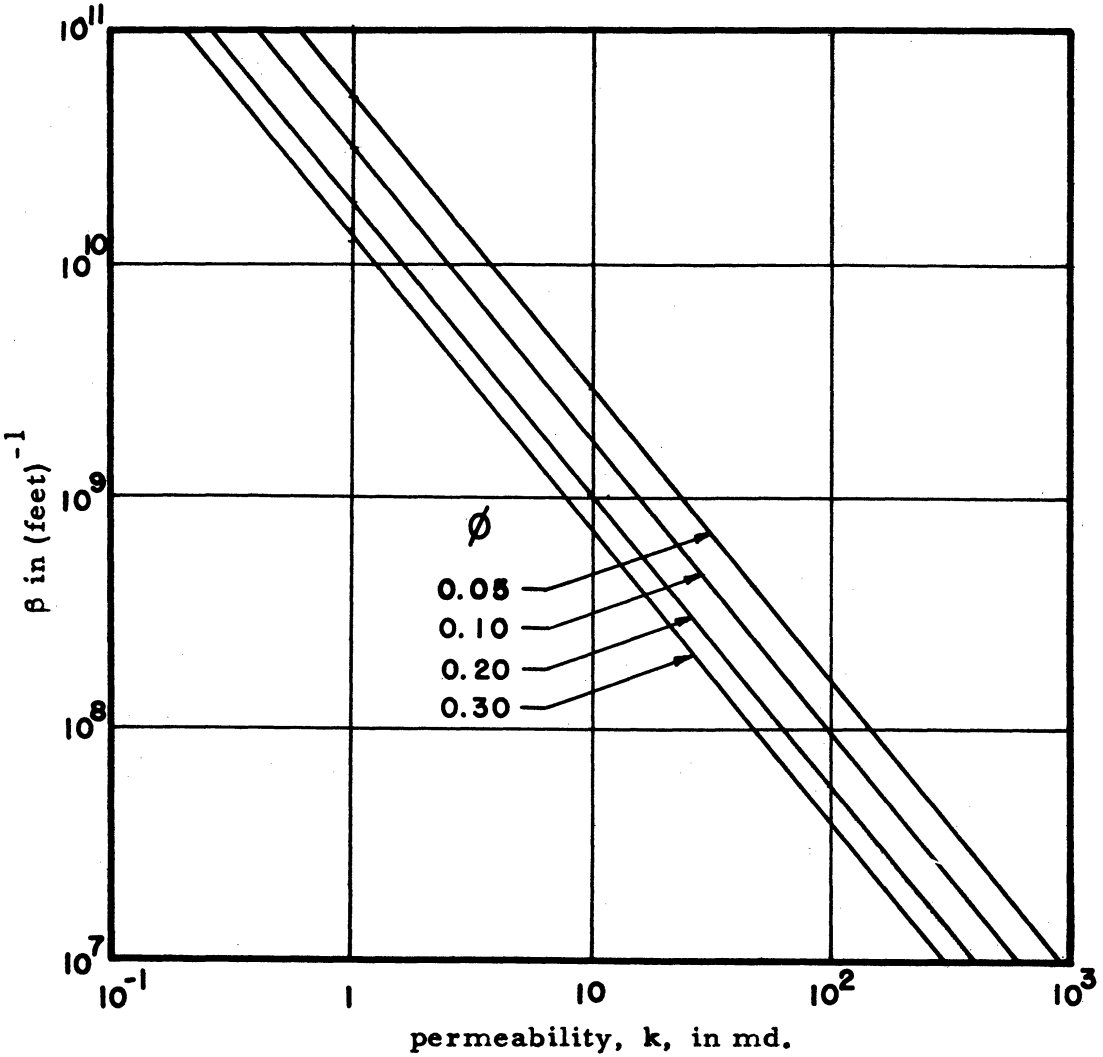


Figure 18. Correlation of β with Permeability k, and porosity, ϕ, for correction of Deviations from Darcy's Law.

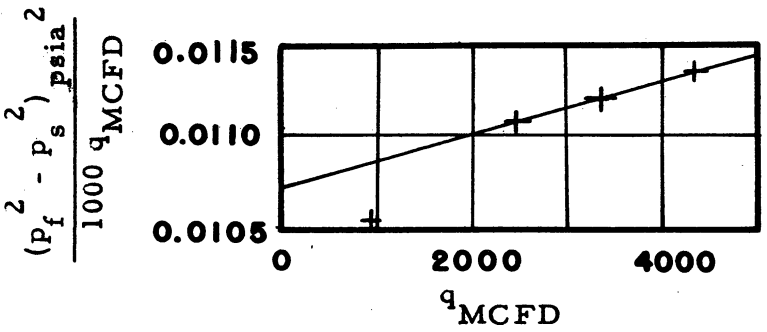


Figure 19. Graph for Evaluation of Constant C in the Quadratic Form of the Back Pressure Equation

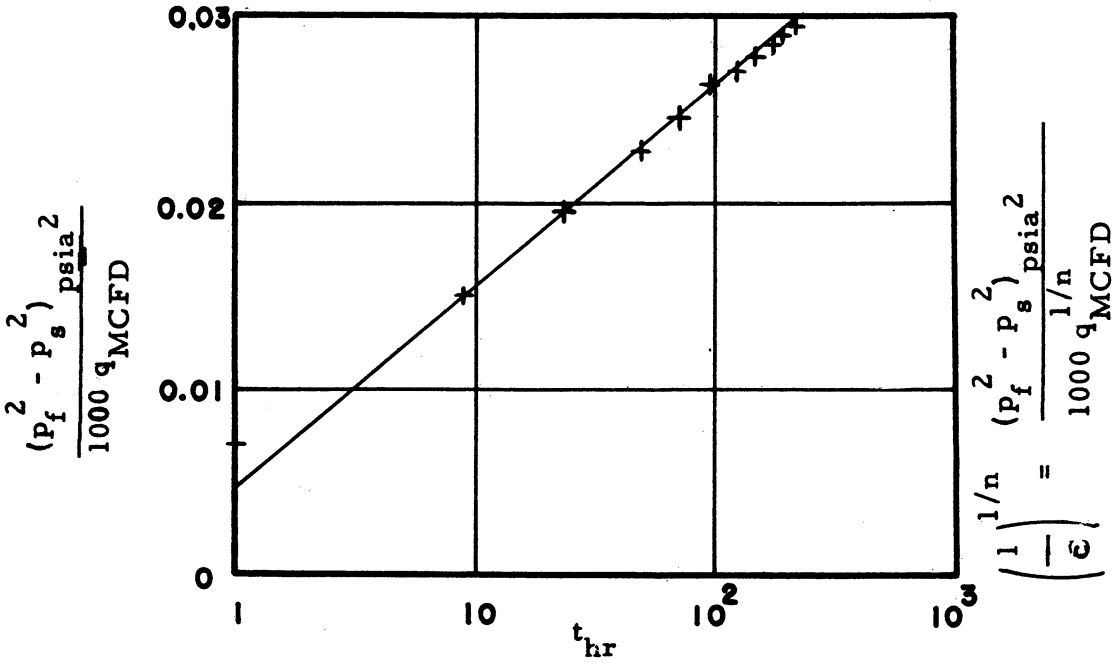


Figure 20. Graph for Evaluation of Constants A and B in the Quadratic Form of the Back Pressure Equation

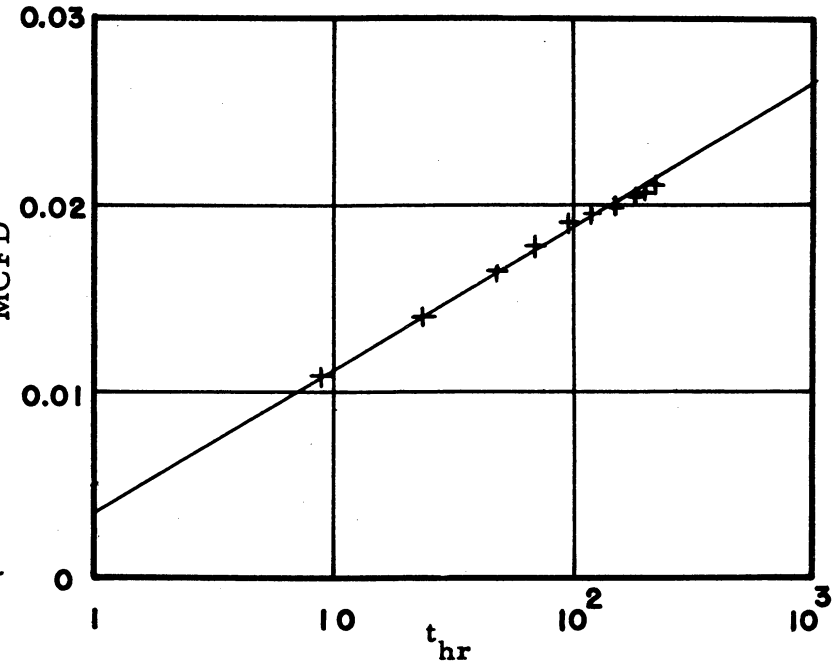


Figure 21. Graph for Evaluation of Constants (λA) and B in the Exponential Form of the Back Pressure Equation

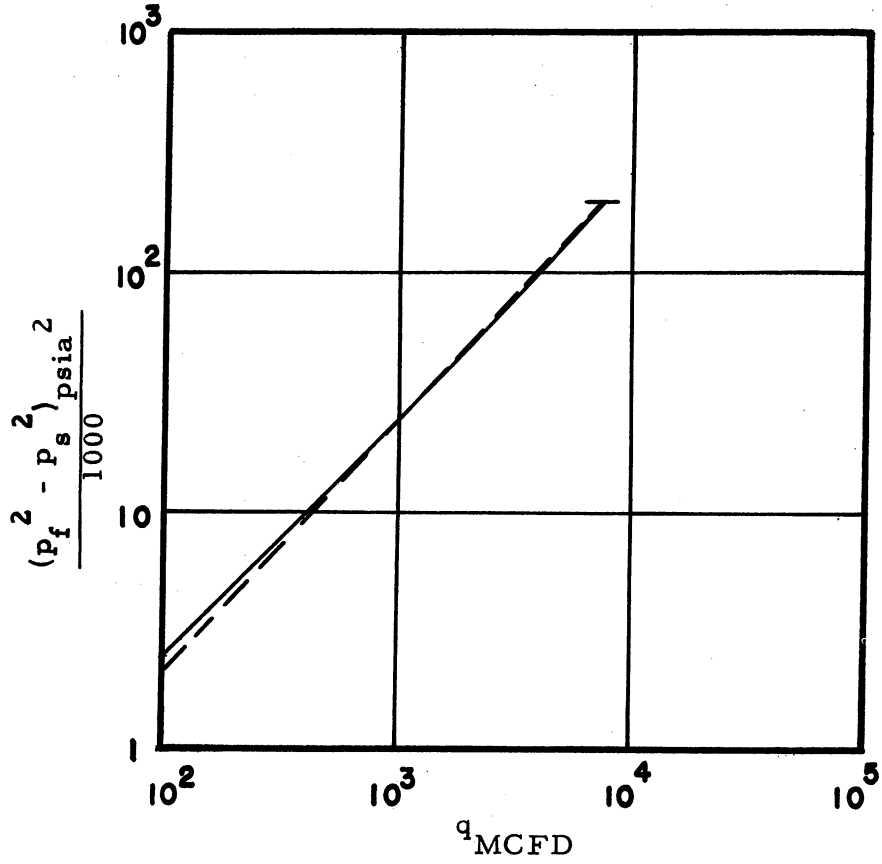


Figure 22. 72 Hour Isochronal Pressure Curves Computed Using Constants Derived from Test Data. Dotted Curve from Exponential Equation and Solid Curve from Quadratic Equation (p_f = 441 psia)

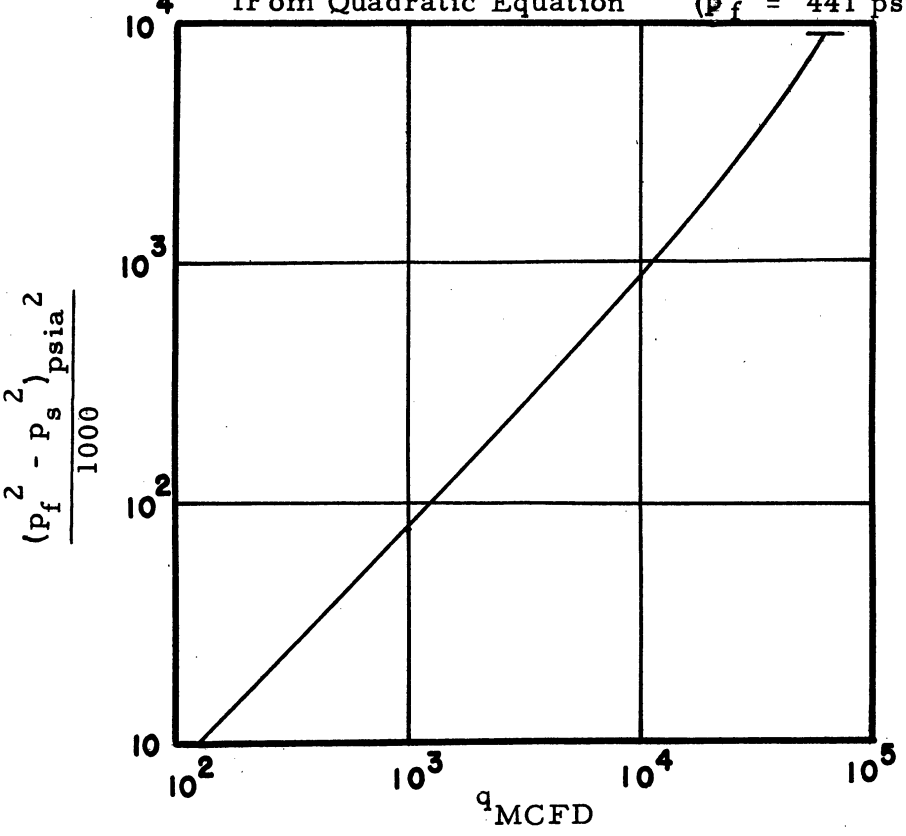


Figure 23. Three-hour Isochronal Back Pressure Curve Computed from Core Data

ERRATA

APPLICATIONS OF UNSTEADY STATE GAS FLOW CALCULATIONS

John D. Janicek and Donald L. Katz

1. Page 7, Equation (13a), for "μC_p" read μ_{cp}.
2. Page 10, line 12 from bottom, for "Figure 3" read "Figure 4".
3. Page 12, Equation (20), for " $\frac{dP^2}{d(\ln r)} = 0$ " read " $\frac{d P^2}{d(\ln R)} = 0$ ".
4. Page 21, line 5 from top, for "Matthews" read "Matthews, Bronz, and Hazebrook."
5. Page 31, line 5 from bottom, for "Cullendar" read "Cullender."
6. Page 40, line 5 from top, for " $(p_f^2 - p^2)/Q$ " read "$(P_f^2 - P^2)/Q$ ".
7. Page 41, in definition of D, for "$D = r_a/r_s$ " read " $D = r_a/r_e$ ".
8. Figure 17, abscissa should read

$$\ln \frac{8 D^2 P_c Q_1}{R_s^2} = \ln D^2 \frac{r_{el}^2}{r_s^2} = \ln \frac{r_{al}^2}{r_s^2}$$

UNIVERSITY OF MICHIGAN
3 9015 03024 6725